Volume 2
Number 20
21 October 2021
Pages 6457–6734

Materials Advances

rsc.li/materials-advances

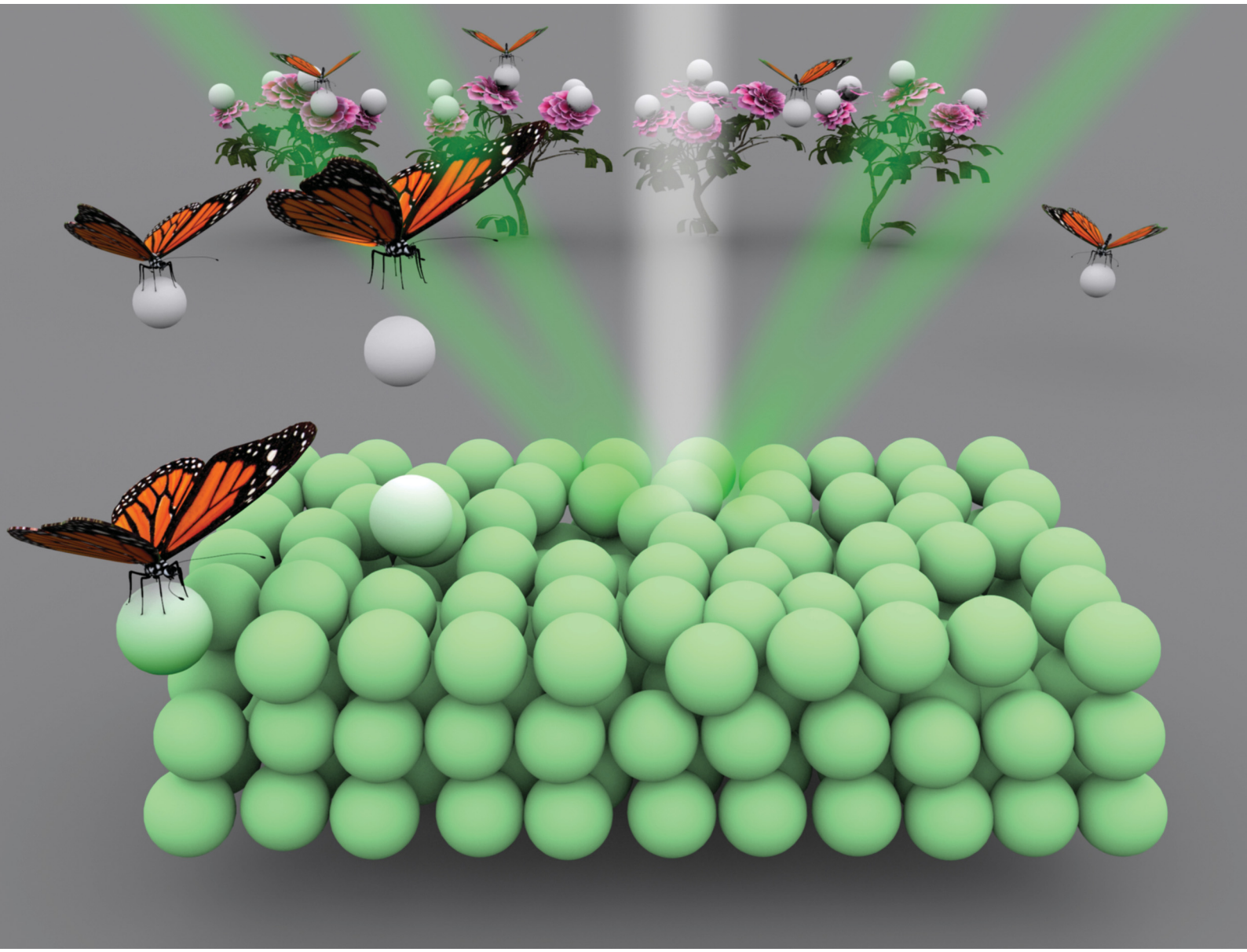

ISSN 2633-5409

ROYAL SOCIETY OF CHEMISTRY

REVIEW ARTICLE
Dongpeng Yang, Shaoming Huang *et al.*
Self-assembly of colloidal particles into amorphous photonic crystals

Materials Advances

ROYAL SOCIETY OF CHEMISTRY

REVIEW

View Article Online
View Journal | View Issue

Cite this: *Mater. Adv.*, 2021, 2, 6499

Self-assembly of colloidal particles into amorphous photonic crystals

Yang Hu‡,[a] Yuqi Zhang‡,[b] Dongpeng Yang,*[a] Dekun Ma[c] and Shaoming Huang*[a]

Received 30th May 2021,
Accepted 3rd August 2021

DOI: 10.1039/d1ma00477h

rsc.li/materials-advances

Colloidal photonic crystals (PCs) have been extensively investigated since they can be prepared in an efficient and low-cost way. Different from the conventional PCs with highly ordered structures, amorphous photonic crystals (APCs) with an isotropic photonic bandgap and non-iridescent structural colors have attracted growing interest especially in pigments, angle-independent displays, and optical coatings. This review focuses on the various strategies used for the fabrication of APCs by spraying, infiltration, layer-by-layer deposition, electrolyte-induced assembly, electrophoretic deposition, phase separation, assembly of bi-disperse-suspension, assembly of particles with a rough surface, assembly of soft particles, and assembly of low-charged particles. Their potential applications are also summarized, such as angle-independent displays, sensors, paintings, anti-counterfeiting labels, information storage, and so on. Finally, we present our perspectives together with the challenges of APCs.

1. Introduction

Photonic crystals (PCs) can be considered as a periodic arrangement of regularly shaped materials (often a multiplicity of layers or spheres in a host polymer) with different dielectric constants.[1,2] Visible light can be selectively reflected by the microstructures of PCs, which can be explained by Bragg's law, resulting in iridescent or non-iridescent structural colors. According to their structures, PCs can be divided into highly ordered and amorphous photonic crystals (OPCs and APCs). OPCs with angle-dependent structural colors have been reviewed by some nice works.[3–9] APCs consist of short-range-ordered colloidal crystals (Fig. 1a); a photonic band structure does not exist and they only have a nonzero photonic density of states photonic pseudogap.[10] As shown in Fig. 1b, the radial distribution function in the APCs with randomly close-packed colloidal particles is almost constant over a large distance range and only has distinct peaks at small distances, which indicates the short-range ordered structure of the APCs. In addition, the ring pattern of the 2D Fourier transform demonstrates the isotropic and short-range ordered structure. The photonic

[a] *School of Materials and Energy, School of Physics and Optoelectric Engineering, Guangzhou Key Laboratory of Low-Dimensional Materials and Energy Storage Devices, Guangdong University of Technology and Synergy Innovation Institute of GDUT, Guangzhou 510006, P. R. China. E-mail: dpyang@gdut.edu.cn, smhuang@gdut.edu.cn*

[b] *Laboratory for Advanced Interfacial Materials and Devices, Institute of Textiles and Clothing. The Hong Kong Polytechnic University, Hong Kong SAR, China*

[c] *Zhejiang Key Laboratory of Alternative Technologies for Fine Chemicals Process, Shaoxing University, Shaoxing 312000, P. R. China*

Yang Hu‡

Yang Hu is currently a PhD candidate at the Collaborative Innovation Center of Advanced Energy Materials at Guangdong University of Technology under the supervision of Dr Dongpeng Yang and Prof. Shaoming Huang. His current research interests are on responsive colloidal photonic crystals and their applications in displays, sensors, and anti-counterfeiting.

Yuqi Zhang‡

Yuqi Zhang received her BSc degree (2012) in applied chemistry and PhD degree (2017) in inorganic chemistry from Tongji University, and postdoctoral training from The Hong Kong Polytechnic University from 2018 to 2021. Her research interests include colloidal photonic crystals, smart sensors, and wearable devices.

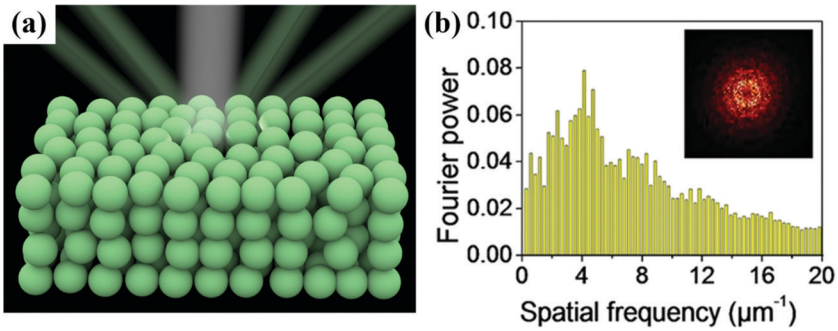

Fig. 1 (a) Schematic of an amorphous colloidal array under white light, and the structural colour from the amorphous array remains nearly unchanged depending on the viewing angle. (b) Histogram of two-dimensional RDF of the APC structure; inset is the 2D Fourier transform. (Reproduced with permission.[36] Copyright 2018, American Chemical Society.)

pseudogaps in APCs are independent of the direction, so they scatter light uniformly in all directions.[11] The coherent scattering of light by an isotropic photonic pseudogap creates non-iridescent structural colors.[12–15] Due to their unique structure, APCs show great potential for application in various fields such as sensors,[16–32] printing,[33–39] displays,[17,30,40–50] and anti-counterfeiting.[45,51–57]

Diverse fabrication methods of APCs by the self-assembly of colloidal nanoparticles have been widely developed in the past decade. Among them, most of the bottom-up strategies are simple and cost-effective. In general, the monodispersed colloidal building blocks have a strong tendency to crystallize,[58,59] and the preparation of APCs by the commonly used self-assembling methods for conventional colloidal crystals is difficult. The key strategy to obtain amorphous colloidal crystals is to inhibit the crystallization of colloidal particles in a large scale or to disturb the self-assembling process of colloidal particles into a partially ordered arrangement. For example, APCs are prepared by the assembly of colloidal particles in multiple sizes.[48,49,60–66] The monodispersed colloidal particles are assembled into amorphous photonic crystals by the following methods: surface modification, concentration of building blocks,[67–69] solvent evaporation,[44,45,70–74] addition of an electrolyte,[75–77] and electrophoretic deposition.[33,34,78–80] In order to reduce the strong incoherent light scattering in the APC structure, light-absorbing

Dongpeng Yang

Dongpeng Yang received his PhD in inorganic chemistry from Fudan University in 2017. He is an associate professor at Guangdong University of Technology since 2017. His current research interests focus on the self-assembly of colloidal particles into smart photonic crystals and extending their applications in color display, pigments, printing, sensing, photocatalysis and anti-counterfeiting.

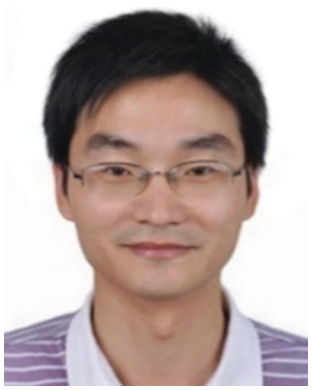

Dekun Ma

De-Kun Ma received his PhD from University of Science and Technology of China in 2007. He studied as a visiting scholar at Domen–Kubota Lab, Tokyo University, Japan during 2012–2013. He was promoted as professor in Wenzhou University in 2015. Five years later, he moved to Shaoxing University and became a full professor in the College of Chemistry and Chemical Engineering. Now he is the director of Zhejiang Key Laboratory of Alternative Technologies for Fine Chemicals Process. He has been working in the research area of photo-functional materials for over 12 years. His current research interests focus on photocatalysis, photoelectrochemical cells, photonic crystals, and electrocatalysis.

Shaoming Huang

Shaoming Huang is a distinguished professor and director of the Collaborative Innovation Center of Advanced Energy Materials at Guangdong University of Technology. He received his BS and MS degrees in Physical Chemistry from Hangzhou University in 1985 and PhD degree in Chemistry from Nankai University in 1991, respectively. His research interests mainly focus on the synthesis and properties of nanostructured carbons and their applications in energy conversion and storage devices.

materials are induced into the amorphous colloidal crystal array to enhance the saturation of their structural color, such as carbon black (CB),[44,81–83] graphene,[21,32,84] polydopamine (PDA),[26,85–87] Fe_3O_4,[17,19,41] and the other commonly used light-absorbing materials.[49,65] In addition, by combining the non-iridescent structural colors of APC arrays with responsive materials, APC devices with different functions can be achieved. However, the commercialization of APCs remains a challenge.

Herein, we summarize the construction strategies for APCs, the light-absorbing materials for improving structural color and their applications. First, a brief overview of the preparation strategies for APCs by self-assembly of colloidal particles is presented, including spraying, infiltration-induced colloidal assembly, layer-by-layer deposition, phase separation, electrophoretic deposition (EPD), space confinement, microfluidic assembly, electrolyte induced assembly, assembly of bi-dispersed-suspension, assembly of rough-surface particles, assembly of soft particles, assembly of low-charged particles and assembly of polymer-grafted particles. Second, the light-absorbing materials applied for eliminating the incoherent light scattering from colloidal amorphous arrays are summarized. Third, the applications of APCs in sensors, printing, displays, and anti-counterfeiting are discussed. Finally, the perspectives and challenges regarding APCs are proposed. This review provides critical insights for the preparation of novel APCs and the extension of their applications.

2. Construction strategies for APCs

2.1 Spraying of colloidal solutions

Spraying of colloidal solutions is an efficient and productive strategy for the rapid assembly of colloidal particles into the APCs by volatilizing the solvents. When a colloidal suspension passes through a nozzle, the building blocks in the droplets rapidly assemble into APCs due to the concentration of the particles by volatilization of the solvent and the wetting of the substrate.[88–91] Takeoka *et al.* prepared APCs with non-iridescent structural colors by spraying a suspension on glass plates using spherical silica particles as the building blocks and methanol as the dispersion medium (Fig. 2d).[44] When the nozzle was too close to the substrate or when a non-volatile solvent was used, the colloidal particles will be assembled in the long-range order with iridescent structural colors.[92,93] Due to the strong incoherent scattering in the APC array, the entire visible light is scattered rendering the APCs white. The black material can absorb the whole visible light to suppress incoherent scattering, and a small amount of black material can be added to the array of APCs in order to obtain a uniform color saturation with a high structural color.[94–96] Takeoka *et al.* added CB to the silica suspension for preparing the APCs, which leaded to the decreasing of baseline of their reflectance spectra. However, their peak intensity remained almost constant, and the color saturation gradually increased with higher proportion of CB.[44] Once this APC film is wetted, the structural color disappears due to the match of refractive index between the particles and the gap. Therefore, Yang *et al.* prepared non-iridescent structural color membranes with superhydrophobicity (static water contact angle of $\sim 155^\circ$ and roll-off angle of $\sim 2^\circ$) by spraying monodispersed fluorosilane-functionalized silica particles (Fig. 2a and b).[45] In addition, Yang and co-workers demonstrated that low surface tension of the particles and the moderate volatility of the solvents were two critical factors in the formation of amorphous arrays in the spraying method, which was acquired by studying the coffee-ring effect on the assembly of colloidal particles.[71] Besides using hydrophobic colloidal particles as the building blocks,[35,45] spraying a hydrophobic solution on an array of APCs is also a commonly used strategy to prepare hydrophobic APCs.[37,73,97] Different from the above, Wang *et al.* developed a method to assemble underwater superoleophobic APC films

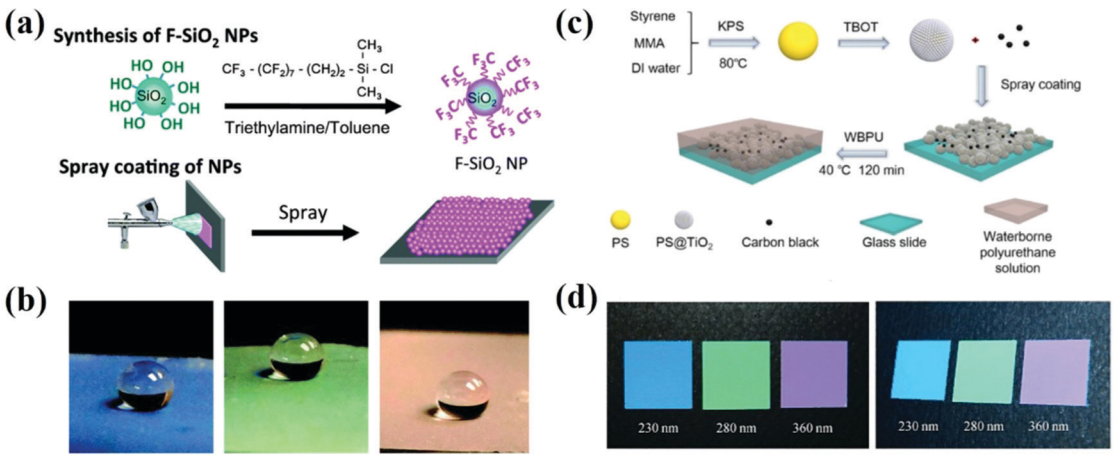

Fig. 2 (a) Schematic illustration of the spraying method. (b) Water droplets ($\sim$10 μL) sprayed on the colorful APC films which are constructed using the spraying method. (Reproduced with permission.[45] Copyright 2014, The Royal Society of Chemistry.) (c) Schematic illustration of the fabrication of the PS@TiO_2 NPs/CB amorphous structures (reproduced with permission.[98] Copyright 2019, American Chemical Society) and (d) the corresponding optical photographs of membranes composed of silica particles with the diameters of 230 nm, 280 nm, and 360 nm, along with 1.7 wt% CB. (Reproduced with permission.[44] Copyright 2013, Wiley-VCH.)

with the rough-surface PS@TiO_2 nanoparticles (Fig. 2c).[98] To improve the adhesion of APCs to the substrate and their mechanical properties, highly viscous polymers can be introduced into the suspension,[35,36,38] or the assembled APCs arrays can be cross-linked[89] or immobilized on the substrate for good mechanical properties.[39] Song *et al.* prepared high-brightness non-iridescent structural colors by adding graphene nanosheets containing a small amount of graphene quantum dots to a sprayed colloidal suspension.[21] Graphene can uniformly absorb visible light enabling APCs with high color saturation. Besides this, the matching of the photoluminescence (PL) wavelength of GQDs with the pseudo photonic bandgap of APCs achieves PL enhancement, which increases the intensity of the reflection peaks by 2.3 times by doping GQDs.[21] Zhao *et al.* reported a multishell graphene oxide encapsulated colloidal nanoparticles, and brightly colored APCs were prepared by the spraying method, where the presence of graphene oxide resulted in high color saturation of the patterns.[32] APCs can be prepared briefly and rapidly by spraying the colloidal solution; however, unsuitable pressure and distance of the spraying machine may lead to the formation of PCs. In addition, the volatility, viscosity, and surface tension of the solvent have significant effects on the uniformity and arrangement of the colloidal crystal array, for example, when the surface tension of the solvent is too high to spread on the substrate surface inhomogeneous APCs are formed.

2.2 Infiltration-induced colloidal assembly

Infiltration-induced assembly of colloidal particles enables fast and large-scale printing of non-iridescent structural color. The APCs are assembled with disordered accumulation of colloidal particles on permeable substrates by the rapid penetration of solvent during the filtration process.[99,100] Anodic aluminum oxide (AAO) films with uniform and size-controlled columnar channels can be applied for quantitative analysis of solvent infiltration. Duan *et al.* assembled colloidal particles on AAO membranes using the infiltration-induced process, which was taken as a model to show the assembling process due to the strong downward infiltration flow in the porous channel of AAO. The colloidal particles were adsorbed on the substrate with disordered arrangement due to the lack of a crystallization drive (Fig. 3a).[74] After completely infiltrating the solvent, the colloidal particles eventually arranged in order. Finally, non-iridescent structural color printing was achieved on paper using an inkjet printer with the colloidal suspension as the ink. Duan and co-workers fabricated thin-film APCs which were assembled by spherical/polyhedral metal–organic framework (MOF) colloidal particles.[101,102] Similarly, Chen *et al.* reported a crack-free, arbitrarily bendable film of APCs with a bright structural color prepared by vacuum filtration of colloidal suspension through a reduced graphene oxide-sulfopropyl methacrylate potassium salt (rGO-SPM) substrate (Fig. 3b and c).[16] Graphene oxide composites effectively reduced the reflected light from the substrate. The strategy of infiltration-induced assembly for the preparation of APCs enables the rapid construction of short-range ordered structures, which can be conveniently printed on solvent-absorbing paper with APC patterns using inkjet printers. However, according to the assembly principle, substrates with high infiltration are required and thus the corresponding applications are limited.

2.3 Layer-by-layer deposition

The layer-by-layer method (LBL method) is a prevalent assembly method for precisely controlling the thickness of the thin films by electrostatic interaction in most cases.[103–107] For investigating

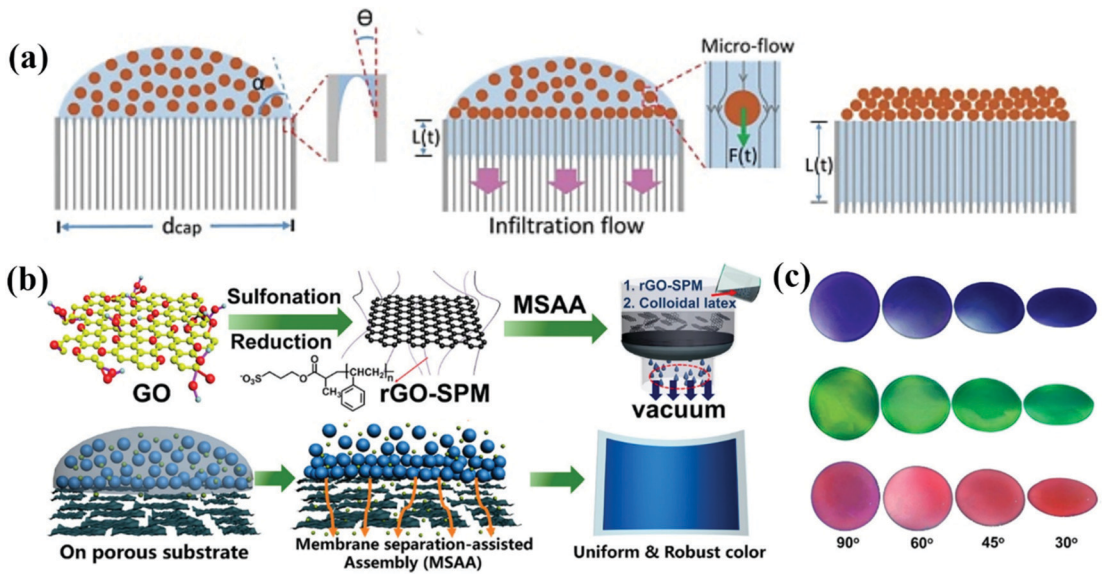

Fig. 3 (a) Illustration of the formation of ACAs due to a strong downward infiltration flow. (Reproduced with permission.[74] Copyright 2018, Wiley-VCH.) (b) Schematic illustration of the fabrication of rGO-SPM and assembly of the rGO-SPM/poly(St-MMA-AA) membranes *via* the membrane separation-assisted assembly (MSAA) method, and Schematic illustration of the MSAA method. The method is facile for achieving uniform structural colors. (c) Photographs of three different colloidal films observed at different angles from 90° to approximately 30°. (Reproduced with permission.[16] Copyright 2019, American Chemical Society.)

the thickness of the APC arrays and the effect of the black material on their optical properties, Takeoka *et al.* prepared large-area and uniform films using charged colloidal particles together with oppositely charged polyelectrolytes in an alternate LBL deposition process (Fig. 4a).[108] The polyelectrolytes with opposite charges on the surface of the substrate are randomly distributed, and therefore the APCs are formed with the disordered packing of colloidal particles under an electrostatic force. They demonstrated that the saturation of the structural color can be improved by controlling the thickness of APCs and using a black substrate, and the blackness of the substrate can be controlled by rotating the orientation of the polarizer. The saturation of non-iridescent structural colors are tunable by controlling the thickness of APC films in the LBL process.[108] The LBL method can precisely control the thickness of APC films by the number of depositions and thus adjust the saturation of non-iridescent structural colors. However, the LBL method has not been widely used for the preparation of APCs because each deposition requires immersion in an oppositely charged solution and harsh assembly conditions.

2.4 Electrolyte-induced assembly

Electrolyte-induced assembly is a method based on the stability theory of charged colloidal suspensions.[109] The electrostatic repulsion between colloidal particles in a suspension system is sensitive to the ions. An electrolyte concentration of 10^{-2} M is sufficient to break the stability of the system, resulting in a disordered arrangement of colloidal particles.[60] Takeoka *et al.* reported a secondary particle in APCs prepared by adding NaCl as the electrolyte (Fig. 4b).[82] When NaCl is added to the suspension, it leads to a decreased thickness of the electric double layer of silica particles and a diminished repulsive force between the particles. Therefore, an amorphous array of closely packed silica particles is formed during solvent evaporation. The addition of CB to the colloidal suspension results in a brighter secondary particle structural color. Subsequently, Takeoka *et al.* prepared monodispersed spherical assemblies using micro-flow-focusing devices and controlled the assembly of silica colloidal particles in the spherical assemblies by the presence or absence of electrolytes, which enabled the spherical assemblies to display iridescent or non-iridescent structural colors (Fig. 4c).[76] In addition, Takeoka and co-workers also reported a method to prepare thin films of APCs by co-assembling a tiny amount of titanium dioxide and silver nitrate with the colloidal suspension of silica. Silver nitrate served as an electrolyte to interrupt the well-ordered assemblies of silica.[75] Electrolyte-induced assembly provides a shortcut for the

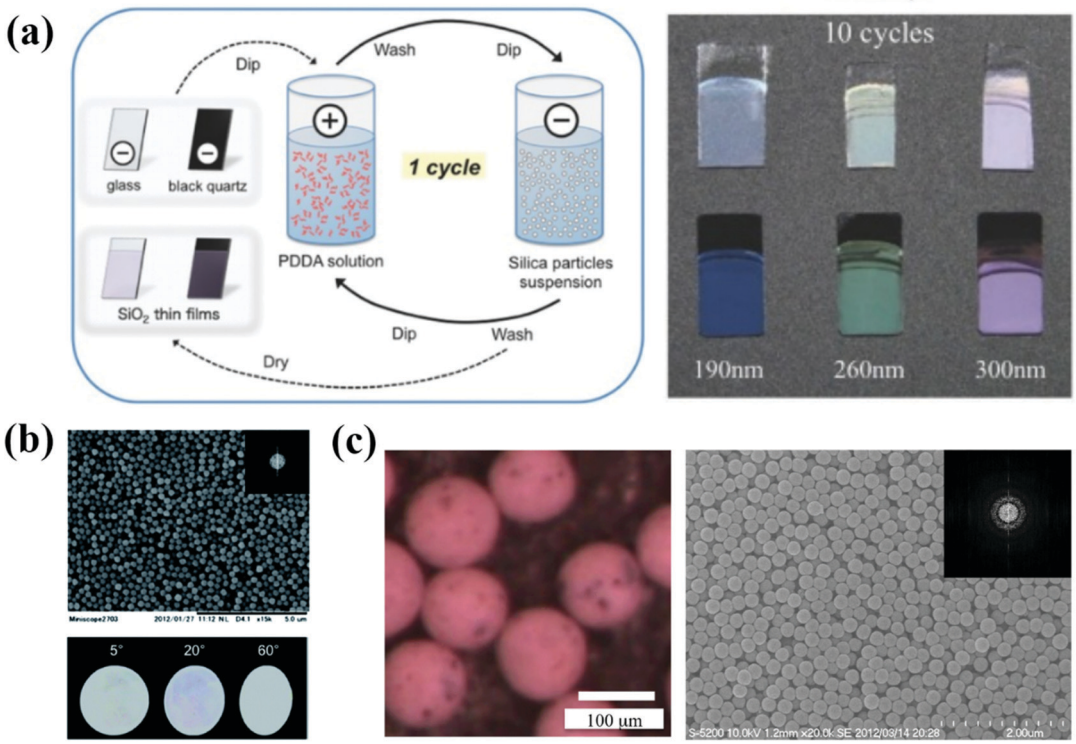

Fig. 4 (a) Preparation method of the colloidal amorphous array composed of silica particles and PDDA on a piece of clear glass plate or a black quartz plate using the LBL method. Optical picture of the colloidal amorphous arrays assembled with different-sized silica particles of 190, 260, and 300 nm and PDDA on a clear glass plate and black quartz plate. (Reproduced with permission.[108] Copyright 2017, Wiley-VCH.) (b) SEM image of the colloidal amorphous array composed primarily of fine spherical silica particles together with a small amount of titanium oxide particles. The insets are a two-dimensional fast Fourier power image obtained from the SEM image and the optical images of the colloidal amorphous array under directional white light in different specular directions. (Reproduced with permission.[75] Copyright 2014, The Royal Society of Chemistry.) (c) A saturated matte SA composed of 310 nm SiO_2 colloidal particles (30 wt% in the aqueous fluid) and magnetite colloidal particles (1 wt% in the aqueous fluid) in air. A SEM image of a matte SA composed of 250 nm SiO_2 colloidal particles. The inset presents the corresponding 2D FFT image. (Reproduced with permission.[76] Copyright 2015, The Royal Society of Chemistry.)

preparation of APCs as a facile approach.[58,110,111] Electrolyte-induced assembly is a simple and facile strategy for the formation of short-range ordered arrangements of colloidal particles *via* destabilizing the colloids by adding electrolytes to the colloidal suspension. However, the lack of sufficient electrostatic repulsion between colloidal particles and their easy precipitation may lead to the formation of APCs with an uneven structural color.

2.5 Electrophoretic deposition

The structure of APCs and PCs can be constructed by applying an electric field between the colloidal suspension and the substrate.[112–117] Kang *et al.* prepared liquid APCs with a tunable structural color by applying different bias voltages on Fe_3O_4@-SiO_2/propylene carbonate suspensions.[41] Fe_3O_4@SiO_2 shows high electrophoretic mobility and high refractive index contrast, allowing liquid APCs to be sensitive to a voltage response and high color saturation. Zhang *et al.* reported a multicolor conductive fiber with APC structure prepared by depositing polystyrene colloidal particles of different sizes on the surface of conductive carbon fibers *via* EPD.[78] In order to solve the problem that structural color fibers cannot be fabricated on a large scale, Zhang *et al.* developed an electrospinning method (Fig. 5a and b).[33] The homogeneity of the electric field during the EPD process directly affects the assembly of colloidal particles. For example, Kang *et al.* reported a method of assembling the dielectric particles in eccentric core–shell microcapsules controlled by dielectrophoresis (DEP) (Fig. 5c), in which the dielectric particles subjected to an inhomogeneous electric field move to the high- or low-field region depending on the dielectric environment.[79] In addition, Takeoka *et al.* successfully constructed structural-color coatings of APCs with silica colloidal particles as the building blocks on conductive substrates by EPD. Co-deposition of CB can reduce the effect of incoherent scattered light on the scattering spectrum and improve the visibility of structural colors. The deposited particles of different sizes produced a variety of brilliant coatings (Fig. 5d), and the evolution of the coating structure from a long-range-ordered arrangement to amorphous packing could be controlled by increasing the deposition voltage.[34] EPD prepared APCs allow precise tuning of the structural color and uniform deposition of colloidal particles by adjusting the bias voltage or changing the size of colloidal particles. In particular, the liquid APCs reported by Kang *et al.* achieve rapid response to voltage and structural color tuning, which provides a new idea for the design of dynamic photonic pixels.[41] However, EPD cannot prepare APCs on nonconductive substrates and power consumption is also a problem.

2.6 Phase separation

The structural-color principle of the barbs on bird feathers in nature inspired the phase separation assembly of APCs.[13] According to Dufresne and Prum *et al.*,[13] the amorphous nanostructures in the barbs are self-assembled by phase separation of β-keratin from the cellular cytoplasm. Polymerization of β-keratin drives phase separation within the cell, and entanglement or cross-linking of β-keratin fibers immobilizes the phase separation structure. Inspired by this assumption, Takeoka *et al.* developed a phase-separated porous polymer membrane with non-iridescent structural color with solvent- and temperature-responsive properties.[118,119] Song *et al.* designed a layered photonic material with the APC structure and deformation-insensitive based on cascade-microphase-separation (CMPS)

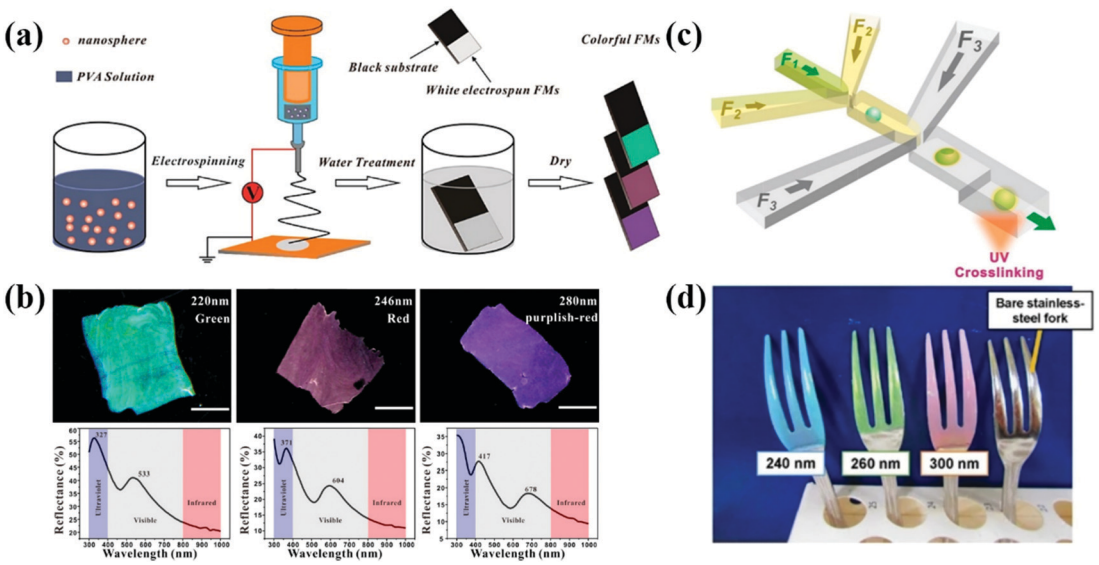

Fig. 5 (a) Schematic illustration of the process of colloidal electrospinning and fabrication of colorful FMs. (b) The optical images of colorful FMs and their corresponding reflective spectra assembled with colloidal spheres with diameters of 220, 246, and 280 nm, respectively. (Reproduced with permission.[33] Copyright 2015, American Chemical Society.) (c) Diagram of a double-flow-focusing microfluidic chip for fabricating the eccentric core–shell microcapsules. (Reproduced with permission.[79] Copyright 2016, Elsevier.) (d) Optical image of polychromatic stainless-steel forks constructed by coating SiO_2 particles with diameters of 240, 260 and 300 nm on forks *via* the EPD process. (Reproduced with permission.[34] Copyright 2017, Springer Nature.)

(Fig. 6a).[120] The lipophilic alkyl-functionalized silica nanoparticles, carbon black, silicone oil and siloxane-based organogels were co-assembled in chloroform. The organogels were crosslinked and gelated by supramolecular hydrogen bonding during solvent evaporation which resulted in microphase separation. The separated silicone oil microdroplets and silica aggregates were immobilized by the gelation and entanglement of supramolecular chains. The silica aggregates were randomly distributed in the composite film, the interior of which consisted of short-range-ordered arrangements of silica particles. Phase separation methods can be used to acquire the structural color bright membrane materials, to impart the ability of APCs to respond to membrane stimuli by introducing stimuli-sensitive polymer systems,[118,119] or to prepare deformation-independent APC composites by using the colloidal particle aggregates formed by phase separation to composites with elastic organogels.[120] However, the phase separation process is time-consuming and complicated and is not suitable for large-scale preparation of APCs.

2.7 Space confinement and microfluidic assembly

A series of functionalized photonic microspheres were prepared by Yang and co-workers based on microfluidic technology.[81,124–128] These photonic spheres show angle-independent structural colors because of the spherical symmetry and their internal structure by long-range ordered packing of colloidal particles.[43,129–134] APC structures can be generated by controlling the volume fraction of the colloidal particles within the photonic microspheres. For example, Kim *et al.* demonstrated an elastic photonic capsule whose optical properties could be controlled by osmotic pressure. The crystallization of the colloidal particles was inhibited by transferring the photonic capsule to an aqueous NaCl solution of high concentration due to a large osmotic pressure difference.[121,135] Accordingly, Manoharan *et al.* fabricated photonic capsules with non-iridescent structural colors by microfluidic techniques with soft-shelled colloidal particles encapsulated in ethoxylated trimethylolpropane triacrylate (ETPTA) and concentrating the suspension with an osmotic pressure gradient (Fig. 6b).[122] Photonic capsules with the APC structure possess a more uniform structural color compared to the colloidal crystal microspheres. In contrast to the above, Song *et al.* utilized a novel "controlled micellization" self-assembly mechanism to achieve non-iridescent structural color microspheres with short-range ordered porous structures (Fig. 6c and d).[123,136–138] Using amphiphilic bottlebrush block copolymers (BBCPs) as the surfactants, the controlled swelling of the reverse BBCP micelles was induced by the confinement of toluene–water microdroplets to make the self-assembled droplets comparable in size to the visible light wavelength. With the evaporation of toluene, short-range ordered porous structures with self-assembled water droplets as templates were formed. Microparticles with non-iridescent structural colors produced by the space confinement and microfluidics techniques show the potential to replace pigments and dyes.[83,139,140] Microparticles with non-iridescent structural colors prepared by space confinement and microfluidic techniques can display vivid structural colors even at lower concentrations, and such assembled APC particles can be used as an alternative to dyes and pigments. However, this strategy

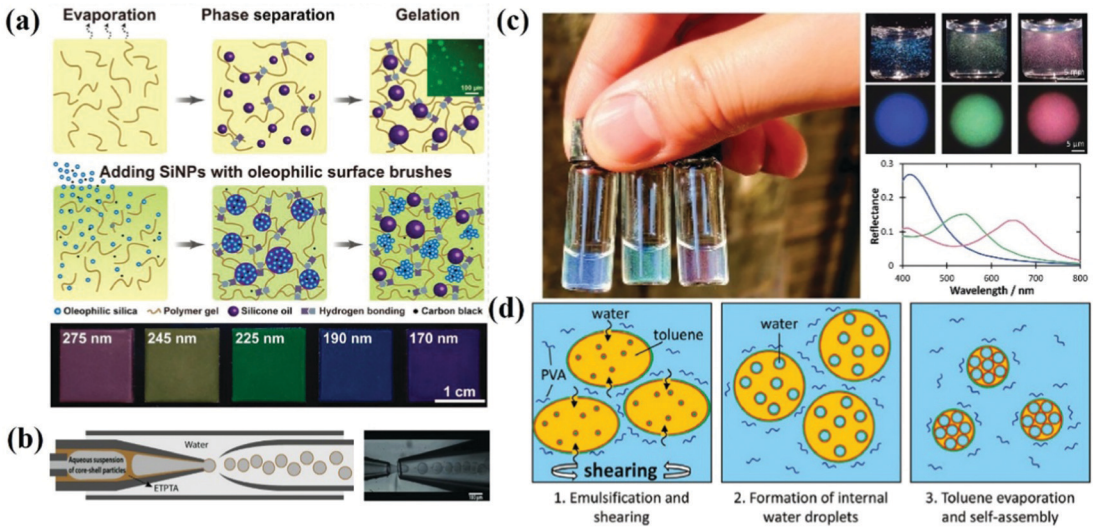

Fig. 6 (a) Schematic illustration of the microphase separation of silicone oils in the hydrogen-bonded supramolecular organogel. Inset shows the microscale droplets of silicone oil incorporated in the organogel, and schematic demonstrates the CMPS process producing the hierarchical photonic structures. The marked numbers represent the diameter of SiO_2 NPs. (Reproduced with permission.[120] Copyright 2019, Wiley-VCH.) (b) Scheme of a capillary microfluidic device for the production of W/O/W double-emulsion droplets with a thin ethoxylated trimethylolpropane triacrylate (ETPTA) membrane. (Reproduced with permission.[122] Copyright 2014, Wiley-VCH.) (c) Left: Aqueous dispersions of blue, green, and red BBCP photonic pigments, illuminated under natural sunlight. Right: Photographs showing the same 0.03 wt% dispersion under direct illumination, and microscopy images of individual microspheres collected under epi-illumination. Corresponding reflectance spectra for the microspheres shown in (c). (d) Schematic illustration of the formation of porous, inverse photonic glass microspheres from an evaporated toluene-in-water emulsion containing the amphiphilic P(PS-NB)-*b*-P(PEO-NB) BBCP. (Reproduced with permission.[123] Copyright 2020, Wiley-VCH.)

generally involves a complex preparation process by microfluidics, and the preparation efficiency remains a challenge.

2.8 Assembly of bi-disperse-suspension

The assembly of bi-disperse-suspension is a common method for preparing APCs, and the assembly of the mixed colloidal particles in two sizes ensures the formation of the APC structure.[51,61,141–146] Takeoka *et al.* obtained APCs with non-iridescent structural colors by the self-assembly of monodisperse silica colloidal particles of two different sizes.[62] Recently, a simple method to systematically control the degree of structural ordering of colloidal photonic crystals and APCs based on adjusting the size contrast of binary particles was proposed by Kim and co-workers (Fig. 7a).[147] At a two particle size contrast of 0.13, the long-range ordered bi-disperse array exhibited high reflectivity and narrow reflection peaks. A short-range ordered structure was established when the size contrast was increased to 0.23 (Fig. 7b). In addition, in their discussion regarding the bi-disperse colloidal particles assembled with reverse emulsion and the membranes assembled *via* evaporation, Xiao and co-workers demonstrated that small-sized colloidal particles tended to stay on the surface of microspheres while the synthetic melanin particles preferred the microsphere surface over silica particles.[148] This work offered a new pathway to the assembly of colloidal particles with different particle sizes and different particle chemistries. The structure of APCs can be created by controlling the coefficient of variation (CV) of the colloidal particle diameters.[41,149,150] For example, Kohri *et al.* prepared APCs with bright non-iridescent structural colors by assembling polydopamine (PDA) particles in CV around 4.4–7.8% (Fig. 7c).[48]

The structure of APCs can be acquired by introducing an additive into the monodisperse suspension.[66,151,152] Zi *et al.* proposed a strategy to prepare APCs by mixing monodisperse polystyrene particles and ink particles of cuttlefish for self-assembly; cuttlefish ink particles are introduced into colloidal suspensions for assembly for absorbing incoherent scattering and disrupting the long-range ordered structure of the colloidal particles.[49] Kim *et al.* reported a strategy for preparing the mechanochromic photonic films by the co-assembly of silica particles, poly(ethylene glycol) phenyl ether acrylate and polydopamine particles (Fig. 7d).[153] In this system, the repulsive force between the neighboring silica particles caused by the solvation layer results in the formation of colloidal crystal arrays. As the concentration of polydopamine particles increases, the interaction of polydopamine on the surrounding colloidal particles inhibits the crystallization of silica particles and therefore a short-range-ordered arrangement structure is gradually formed. APCs were prepared easily and rapidly by bi-disperse-suspension assembly, and the transformation from the PC to APC structure could be achieved by adjusting the size contrast of binary particles.[147,153] However, it is necessary to alter the size of binary particles and the ratio of each component when adjusting the structural color, which is a tedious process.

2.9 Assembly of particles with a rough surface

The rough-surface colloidal particles assist in the assembly of the APC structures. Yang *et al.* grafted polypyrrole (PPy) particles onto the surface of polystyrene nanoparticles by *in situ* polymerization, which led to the formation of amorphous arrays due to the bumpy surface of the core–shell nanoparticles (Fig. 8a and b). The black PPy shells provided strong contrast in the APCs by suppressing incoherent scattering and multiple light scattering.[154] In addition, Yang *et al.* reported colloidal particles consisting of PPy shell and silica core, which can be directly used to prepare APCs by dispersion in a solvent. The surface grafted polypyrrole effectively suppressed the coffee-ring effect during drying of the colloidal suspension.[155] Similarly, Kohri *et al.* used polydopamine (PDA)-coated polystyrene (PS) as the building blocks and created a highly visible structural color with an APC structure by controlling the thickness of the PDA shell

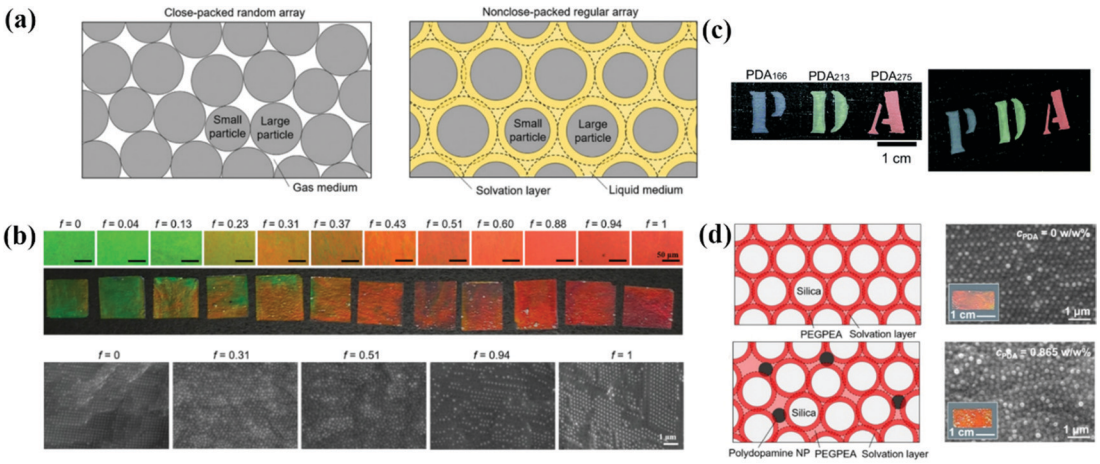

Fig. 7 (a) Schematic illustrations showing the arrangement of the colloidal particles with two different diameters. (b) Optical microscopy (OM) images and optical images of photonic films prepared with various volume fractions of large particles. Cross-sectional SEM images of the films at different volume fractions. (Reproduced with permission.[147] Copyright 2019, Wiley-VCH.) (c) Photographs of photonic films constructed using black PDA particles. (Reproduced with permission.[48] Copyright 2015, The Royal Society of Chemistry.) (d) Polydopamine nanoparticle-loaded non-close-packed colloidal arrays in the elastic matrix. (Reproduced with permission.[153] Copyright 2019, American Chemical Society.)

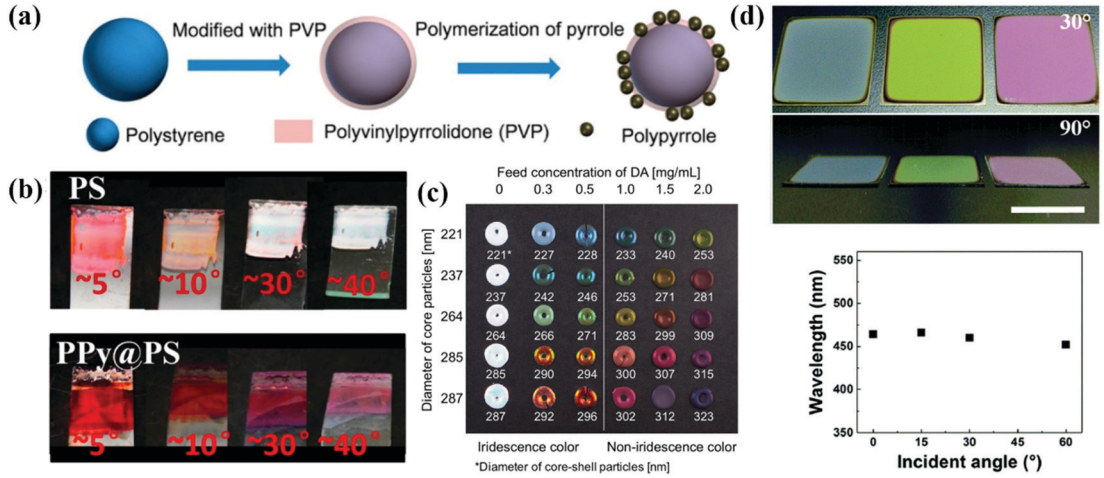

Fig. 8 (a) Schematic illustration of the modification of PS NP with PVP. (b) Photographs of films assembled with PS and PPy@PS NPs observed from different angles. (Reproduced with permission.[154] Copyright 2016, American Chemical Society.) (c) Structural color pellets of PSt(X)@PDA(Y) core–shell particles. (Reproduced with permission.[156] Copyright 2014, Springer Nature.) (d) Photographs of crack-free PS@PDA/APTES hybrid PC films observed from different viewing angles. Relationship between peak wavelengths from the reflection spectra and the incident angle. (Reproduced with permission.[157] Copyright 2017, The Royal Society of Chemistry.)

which decides the surface roughness of the colloidal particle of PS@PDA (Fig. 8c).[156] Sheng *et al.* co-assembled PS@PDA nanoparticles with 3-aminopropyltriethoxysilane (APTES) and managed to counteract the tensile stress caused by the shrinkage of the colloidal suspension during drying due to the generation of covalent bonds between PDA and APTES, addressing the cracking problem during the preparation of APCs (Fig. 8d).[157,158] The utilization of surface roughness of the assembled particle can simplify the preparation process to obtain APCs of high quality.[159–163] High-quality APCs can be prepared with surface rough particles, which are not constrained by substrates and solvents, and the rough black viscous shell improves the light absorption efficiency and adhesion properties of the particles to the substrate.[89,157] However, the modification of a certain thickness of rough shell on smooth colloidal particles is not easily controlled, which limits their large-scale synthesis.

2.10 Assembly of soft particles

The high viscosity of the particles during the assembly of soft particles leads to interparticle adhesion and a significant decrease of the assembling efficiency, which results in the formation of APC structures.[67,164,165] By assembling the *N*-isopropylacrylamide-derivative nanoparticles into hydrogel opal, Hu *et al.* demonstrated that the nanoparticles self-assembled into a short-range-ordered glass phase when the concentration is more than 5 wt%.[67] Subsequently, Hu and Gao discussed the assembly of *N*-isopropylacrylamide (NIPA) gel particles in water and revealed that the NIPA gel particles endured a phase transition from a liquid to glassy state through crystal at room temperature as the NIPA concentration increased.[68] Takeoka *et al.* reported that the structural color by amorphous assembly of charged spherical particles is angle-independent and responds rapidly to temperature changes (Fig. 9b).[69] The liquid APC system is promising as the display material with non-iridescent and permanently non-fading features.

Amorphous arrays can also be realized by constructing colloidal particles with a hard-core and soft-shell as the assembly blocks. Takeoka *et al.* prepared poly(N-isopropylacrylamide) (PNIPA) coated silica particles in a core–shell structure whose diameter is variable with water temperature.[166] The soft PNIPA shell is bonded and retains the thermal response, so that the optical properties of APCs assembled from the core–shell particles reversibly depend on temperature. Manoharan *et al.* synthesized colloidal particles composed of a polystyrene core and a poly (*N*-isopropylacrylamide-*co*-acrylic-acid) shell in a similar way and assembled them as the APC membranes (Fig. 9a).[42] The non-iridescent photonic pigments in the visible range were prepared by Manoharan *et al.* The pigments can weaken multiple scattering by using microfluidic techniques to encapsulate the colloidal particles in spherical capsules.[122] The APCs assembled by colloidal particles coated with soft polymer shells exhibit weak incoherent scattering and bright structural colors. And the assembly of particles with temperature-sensitive polymer shells can be used to obtain APCs with a temperature response.

2.11 Assembly of low-charged particles

Colloidal particles with a surface-grafted polymer tend to form short-range-ordered arrangements during assembly due to reduced electrostatic repulsive forces.[18,168–171] Watanabe *et al.* prepared arrays of soft glassy APCs with ionic conductivity by dispersing poly(methyl methacrylate) (PMMA)-grafted monodispersed silica colloidal particles in ionic liquids (Fig. 9d).[40] Then, they investigated in detail the relationship among colloidal glass transition, ion transport and structural color in this system. They demonstrated that the soft glassy colloidal arrays underwent glass transition at a higher volume fraction than the one in the hard sphere systems and the APCs had higher ionic conductivity in the high concentration region.[172] Moreover, they also reported the assembly of thermosensitive poly(benzyl methacrylate) (PBnMA)-modified silica particles in

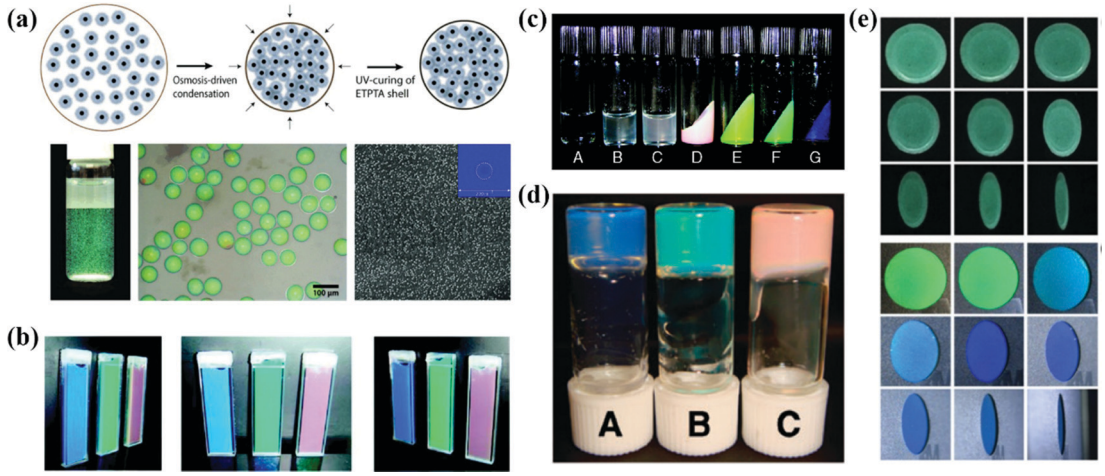

Fig. 9 (a) Schematic illustration of the osmosis-driven condensation process. The optical image and optical microscope image of the photonic pigment in water after UV-curing of the ETPTA shell. SEM image of the particles. (Reproduced with permission.[122] Copyright 2014, Wiley-VCH.) (b) Optical images of gel suspensions with different polymer contents. (Reproduced with permission.[69] Copyright 2009, American Chemical Society.) (c) Appearance of PMMA- and PBnMA-grafted silica colloidal suspensions. (Reproduced with permission.[167] Copyright 2010, American Chemical Society.) (d) Photograph of soft glassy colloidal arrays in an IL at different particle concentrations. (Reproduced with permission.[40] Copyright 2009, The Royal Society of Chemistry.) (e) Digital photos of APCs and OPCs which were assembled from aminated silica particles under different pH values. (Reproduced with permission.[168] Copyright 2020, American Chemical Society.)

ionic liquids, and showed phase separation at lower temperatures over a wider temperature range (Fig. 9c).[167] In the colloidal system assembled using ionic liquids, the presence of ions reduces the electrostatic repulsion between the colloidal particles, while the steric forces and solvation effectively stabilize the colloidal particles.[173] Based on this, Watanabe and co-workers prepared colloidal glasses and gels by assembling grafted polymeric silica particles and unstable silica particles in an ionic liquid.[173] Colloidal glass with an APC structure shows a uniform non-iridescent structural color and fluidic properties that are expected to be used in wide viewing angles for color displays.

When the polymer is incorporated directly into the colloidal suspension, the adsorbed polymer on the colloidal particles results in a closely packed short-range ordered structure.[86,174] Kim *et al.* prepared APCs of uniform thickness by evaporating the solvent from a colloidal suspension of polyethylene oxide (PEO)-coated silica on a heated substrate.[175] The temperature of the substrate allows the generation of Marangoni flow within the droplets of the water–ethanol mixture to inhibit the formation of coffee-rings, and the physical adsorption of PEO on the surface of silica prevents the crystallization of colloidal particles.[175] Kofinas *et al.* reported an assembly strategy of colloidal particles into APC gels by which the protein degrading peptides lead to the adsorption of polymers onto the particle surface.[27] Sheng *et al.* reported an APC with excellent mechanical properties by co-assembling PS@PDA particles with chitosan which plays the role of enhancing the hydrogen bonding networks between the colloidal particles and inducing the assembly of colloidal particles into APCs.[176]

Our group has developed a series of strategies for preparing colloidal particles by controlling their surface charge in the dispersant. First, we synthesized Fe_3O_4@SiO_2 core–shell particles by the *in situ* deposition of Fe_3O_4 nanoparticles on SiO_2 particles. The Fe_3O_4 shell significantly reduces the potential of silica particles and eventually results in a short-range-ordered arrangement of Fe_3O_4@SiO_2 colloidal particles. The absorption of scattered light by the black Fe_3O_4 shell is important for the formation of uniform and bright structural colors.[177] Subsequently, we introduced polyvinylpyrrolidone (PVP) into the silica suspension and prepared APCs by an evaporation induced self-assembling method.[111] The decreased ζ-potential value of silica and particle agglomeration is critical to the formation of amorphous arrays due to the adsorption of silica on PVP during self-assembly. In another work, APCs and PCs were fabricated by co-assembling amidated silica particles and carbon black in an acidic aqueous solution (Fig. 9e).[168] The high concentration of H^+ ions promotes the protonation of particles to produce large ζ-potential values on the silica particles, which facilitates the crystallization of colloidal particles. Therefore, the ordering of the assembled particles can be precisely controlled by adjusting the pH of the colloidal solution. Moreover, we synthesized $YOHCO_3$ particles with tunable size, composition and optical properties before being self-assembled into the APCs.[150] The $YOHCO_3$ colloidal particles were assembled into the amorphous structure by a low surface potential, and the APCs patterned by the Eu^{3+}-doped $YOHCO_3$ colloidal particles presented red under UV irradiation. In the subsequent work, we obtained Y_2O_3(:Eu) by a hydrothermal process *via* the high-temperature calcination of $YOHCO_3$(:Eu) particles. The low surface potential of the particles as well as their high polydispersity contributed to the formation of APCs.[178] The invisible photonic prints with UV irradiation were prepared by assembling Eu-doped and Eu-undoped Y_2O_3 particles. In addition, we reported a novel method to prepare APCs with non-iridescent structural colors by assembling colloidal particles in a less-polar dispersant.[179] Based on the

sensitivity of the APCs to the refractive index contrast, their structural color disappears once the APCs are wetted. Accordingly, we developed an information storage system for water recognition. Our studies have important implications towards the simple and fast large-area preparation of APCs in non-iridescent structural colors and understanding the assembly behavior of colloidal particles in different pH and diverse polar solutions. Generally, there are two ways to obtain low potential colloidal particles, one is by grafting on the surface of the particles and the other is by adding polymers to the colloidal suspension. Both strategies can produce APCs with a uniform structural color, but the former requires further modification of the particles synthetically, which is time-consuming, while the latter can simply and rapidly prepare APCs by merely introducing polymers to co-assemble with the colloidal particles.

3. Applications of APCs

The short-range-ordered structure of APCs generates non-iridescent structural colors and stronger incoherent scattering compared with PCs with a well-ordered arrangement, which provides a unique advantage for potential applications of APCs. For example, for displays and printing, APCs have tunable structured colors covering the entire visible spectrum. More importantly, their structural colors are angle-independent which effectively avoids color confusion. APCs can be embedded in or constructed using responsive materials with optical signals modulated in response to external stimuli, including mechanical deformation,[29,180] temperature,[30,166,170] light,[24,75] humidity,[21,23] magnetic[28,82] and electric fields.[19,41] In addition, the combination of the non-iridescent properties of APCs and iridescent structural colors of PCs provides new ideas for anti-counterfeit labels.[51,178]

3.1 Sensors

APCs offer an effective solution for sensors due to their unique and designable optical properties in response to external stimuli. Zhu *et al.* reported a mechanochromic supramolecular elastomer prepared by immobilizing isotropically arranged SiO_2 in the elastomer of amino-terminated poly(dimethylsiloxane) (amino-PDMS) which is ligated with cerium trichloride metal coordination.[29] As the tensile strain increases from 0 to 120%, the reflection peak of the APCs elastomer shifts from 660 nm to 550 nm along with the shift of the structural color from red to green.[29] They concurrently developed a recyclable APC elastomer prepared by combining short-range-ordered SiO_2 arrays with a water-soluble ureidopyrimidinone (UPy) which is cross-linked with a poly(ethylene glycol) (PEG) polymeric matrix.[181] The reversible cross-linking and water solubility of PEG-UPy polymers confer excellent recyclability to APC elastomers.[181] Recently, they proposed a wide-spectrum responsive APC elastomer assembled with carbon-coated Fe_3O_4 as the building blocks followed by embedding in Amino-PDMS, which exhibits a wavelength difference of $\approx$223 nm during reversible stretching (Fig. 10a).[180] Kim *et al.* prepared mechanically discolored APC elastomers by studying the assembly of bi-dispersed colloidal particles in PEG-PEA resin.[147,153] Some of the APC elastomers with self-healing properties will be fully utilized in colorimetric sensors.[29,180,181]

Takeoka *et al.* prepared APCs by assembling soft particles with a temperature-sensitive shell which caused reversible changes of reflection peaks with temperature.[166] To develop a temperature-responsive chromatic sensor, they constructed the

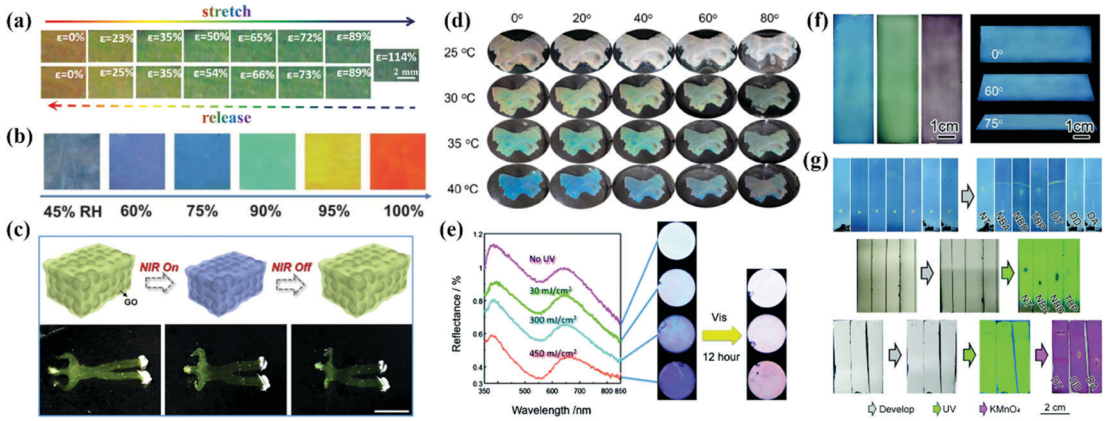

Fig. 10 (a) Photographs of red Fe_3O_4@C/PDMS PE40 by stretching (upper) and releasing (lower) at various strains ranging from 0% to 114%. (Reproduced with permission.[180] Copyright 2020, Wiley-VCH.) (b) Photograph and reflectance spectra of the brilliant structural color sensor at reversible RH variations. (Reproduced with permission.[21] Copyright 2018, Wiley-VCH.) (c) Scheme of the photothermal response of the inverse opaline hydrogel of NIPAM and side views of the shrinking process. Controllable movement of the human-shaped NIPAM hydrogel. (Reproduced with permission.[32] Copyright 2019, Elsevier.) (d) Optical photographs of PM0 in water at a certain temperature from different observing angles. (Reproduced with permission.[24] Copyright 2021, American Chemical Society.) (e) The reflection spectra and the optical images of the amorphous colloidal array with an aqueous solution of silver nitrate under 313 nm UV light passed through a bandpass filter and optical images of the colloidal amorphous array that was irradiated with visible light (λ > 420 nm) for 12 h under the conditions as shown in the left. (Reproduced with permission.[75] Copyright 2014, The Royal Society of Chemistry.) (f) Digital photos of the m-SiO_2 APC films prepared using 236 nm, 276 nm, and 309 nm particles and blue APC films from different viewing angles. (g) Direct recognition of seven chemical compounds on (up) the m-SiO_2 APC film and their recognition on a traditional fluorescent SiO_2 gel plate (middle) under UV light or (bottom) after dyeing. (Reproduced with permission.[182] Copyright 2020, The Royal Society of Chemistry.)

porous PNIPA hydrogels with APC structure by dipping PNIPA into SiO_2 amorphous array templates and removing the templates by etching.[30] Owing to the large proportion of PNIPA in this system, the porous PNIPA hydrogels exhibited rapid volume and structural color changes when the temperature varied.[30] Xia *et al.* reported a hydrogel membrane consisting of the amorphous arrangement of microgels with a dual response for temperature and pH value. The volume phase change temperature of the poly(N-isopropylacrylamide) (pNIPAAm) polymer in water provides thermochromic properties in the hydrogel membrane, while the methacrylic acid provides pH-response to the hydrogel membrane (Fig. 10d).[25]

Xiao *et al.* reported a colorimetric humidity sensor assembled by melanin nanoparticles that produced continuous structural color changes when the relative humidity changed from 10% to 90%. The sensor exhibited excellent cycling performance and high sensitivity at a given humidity level.[23] Song *et al.* infiltrated amide monomers into the templates of APCs to obtain the humidity sensor by UV curing.[23] Its structural color showed a reversible change from blue to red when the relative humidity varied between 45% and 100%. The sensor exhibited structural color changes in different humidity ranges with colloidal particles in different sizes (Fig. 10b).[23] Takeoka *et al.* utilized the photoelectrochemical reaction of Ag/Ag^+ to modulate the intensity of noncoherent scattered light and the variation of saturation in the APC array by light (Fig. 10e).[75] Xia *et al.* developed an APC hydrogel with near-infrared light modulation of color change, which was prepared by packing dry thermosensitive microgels in pNIPAAm and introducing multi-walled carbon nanotubes (MWCNTs).[24] MWCNTs can not only absorb near-infrared light but also convert luminous energy into thermal energy to produce structural color changes in hydrogels.[24] Zhao *et al.* prepared infrared-light-responsive APC hydrogels by infiltrating n-isopropylacrylamide gels into the APCs templated by multi-shell particles.[32] The graphene oxide shell converts the energy of infrared light radiation into heat, which results in volume contraction and self-healing of the APC hydrogel (Fig. 10c).[32] Magnetically responsive APC sensors are usually prepared with Janus particles as the building blocks. For example, Takeoka *et al.* prepared Janus particles composed of SiO_2 colloidal particles and Fe_3O_4 nanoparticles by the microemulsion method. Their orientations could be changed by a magnetic field, and the structural color changed accordingly.[28] To construct an electrically responsive APC sensor,[41] Chung *et al.* reported the APCs self-assembled by $Fe_3O_4@SiO_2$, whose structural color changed from mahogany to dark blue under the voltage ranging from 1.0 to 4.0 V.[19] Recently, Ge *et al.* reported for the first time that a thin layer chromatography (TLC) based on mesoporous silica particle was assembled with high separation efficiency and convenient recognition (Fig. 10f and g).[182] In contrast to the conventional TLC, the large number of micron-sized pores in the APCs greatly enhances the capillary forces and accelerates solvent diffusion. The mesoporous silica APC membranes show uniform non-iridescent structural colors, and the color changes with good distinction during the separation of the analyzed chemical compounds.

3.2 Painting

Full color painting and printing of APC patterns in a large area can be achieved by spray or infiltration-induced assembly. The patterns painted or printed with the inks of APCs are environmentally friendly with low energy consumption and are operational with wide viewing angles. Takeoka *et al.* successfully drew Mt. Fuji by spraying a colloidal suspension of carbon black-doped silica (Fig. 11a).[44] Duan *et al.* developed a large-scale full-spectrum structural color printing technique by infiltration-induced colloidal assembly. The patterns were printed using colloidal inks with a strong solvent absorption capacity.[74] The structural color can be easily tuned using the CMYK mode of a domestic inkjet printer (Fig. 11b). The strong permeability of the paper to solvents ensures the colloidal particles to form APCs on the paper.[74] Gu *et al.* painted robust non-iridescent structural colors of Peking Opera character faces by spraying $SiO_2@PDA$ on different substrates (Fig. 11e).[89] Zhang *et al.* painted the patterns of APCs by spraying a mixed emulsion of thiodiphenol-formaldehyde particles and carbon black on a thermoplastic polymeric film followed by sandwiching the structure to obtain an integrated composite film by hot pressing (Fig. 11d).[39] The APC composite film fully compensates for the lack of mechanical properties of the printed APCs.

Zhang *et al.* proposed a new method to prepare homogeneous APCs on a variety of substrates by atomized deposition of the colloidal suspensions of silica with poly (vinyl alcohol) (PVA) (Fig. 10f).[36] Patterns can be painted on the fabric, and the introduction of PVA improves the adhesion between the APCs and the fabric, maintaining almost the same structural color after stretching, rubbing and washing tests.[36] Shen *et al.* used a mixture of chitosan (CS) and PS@PDA particles for dyeing cotton fabrics, which resulted in a robust coating of PS@PDA/CS on the substrate due to the enhanced bonding of APCs by CS and the bonding of the colloidal particles to cotton fibers.[176] Tang *et al.* added the synthetic aqueous polyureas (WPU) to the APCs assembled with polysulfide colloidal particles to obtain the non-iridescent structural color coatings. The products show high color contrast, favorable mechanical properties and self-healing properties.[38] With WPU as the efficient binder to the gap-locking structure of the amorphous array, this method can be applied for fabric dyeing (Fig. 10c).[38] Zhang *et al.* printed non-iridescent structural colors and structurally stable patterns of APCs on a fabric using a rapid screen printing technique.[174] In addition, our group printed structural color patterns of APCs with multi-color vivid non-iridescent colors by hand-painting and spraying methods (Fig. 10g).[111,150,177]

3.3 Displays

The non-iridescent structural colors make APCs a promising next-generation display device with wide-viewing angles. In the work of Kang *et al.*, they prepared the angle-independent photonic pixels that can vary with voltage.[41] When the bias voltage increased from 1.0 V to 4.0 V, the reflection peak of the

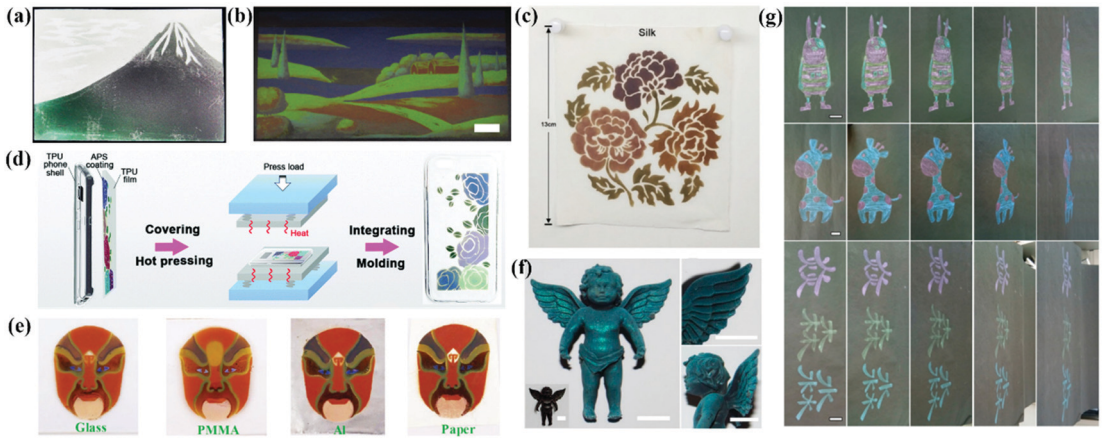

Fig. 11 (a) A picture of Mount Fuji drawn by spraying the suspensions of silica particles and CB. (Reproduced with permission.[44] Copyright 2013, Wiley-VCH.) (b) A multicolored painting of a landscape with high resolution, scale bar: 1 cm. (Reproduced with permission.[74] Copyright 2018, Wiley-VCH.) (c) A complex pattern sprayed with PSFMs and WPU in four different diameters on silk. (Reproduced with permission.[38] Copyright 2019, American Chemical Society.) (d) Schematic diagram of the preparation of TPU composite phone shell with a non-iridescent structural color. (Reproduced with permission.[39] Copyright 2019, The Royal Society of Chemistry.) (e) The multi-color patterns of PDA@SiO_2-AM arrays on glass, PMMA, Al foil and paper. (Reproduced with permission.[89] Copyright 2018, The Royal Society of Chemistry.) (f) Cyan-color dyed toy of angel using silica NPs with a diameter of 212 nm together with 4 wt% PVA (inset, pristine angel toy) and enlarged view. (Reproduced with permission.[36] Copyright 2018, American Chemical Society.) (g) Colorful patterns with blue, green, yellow, and red structural colors obtained by hand painting or writing on paper. (Reproduced with permission.[150] Copyright 2019, American Chemical Society.)

photonic pixel reversibly shifted from 655 nm to 490 nm and the structural color changed from red to blue covering the entire visible region (Fig. 12b).[41] In addition, the photonic pixels have high sensitivity and excellent operating stability. Yang *et al.* reported a smart display window prepared from an array of silica particles composited with poly(dimethylsiloxane) (PDMS) elastomer (Fig. 12a).[183] The elastic film is initially highly transparent due to the matched refractive index of the silica particles and the PDMS. When it is stretched and the strain is greater than 40%, the micro-wrinkles and voids are generated and therefore the transmittance is reduced to 30% and the film shows non-iridescent structural colors.[183]

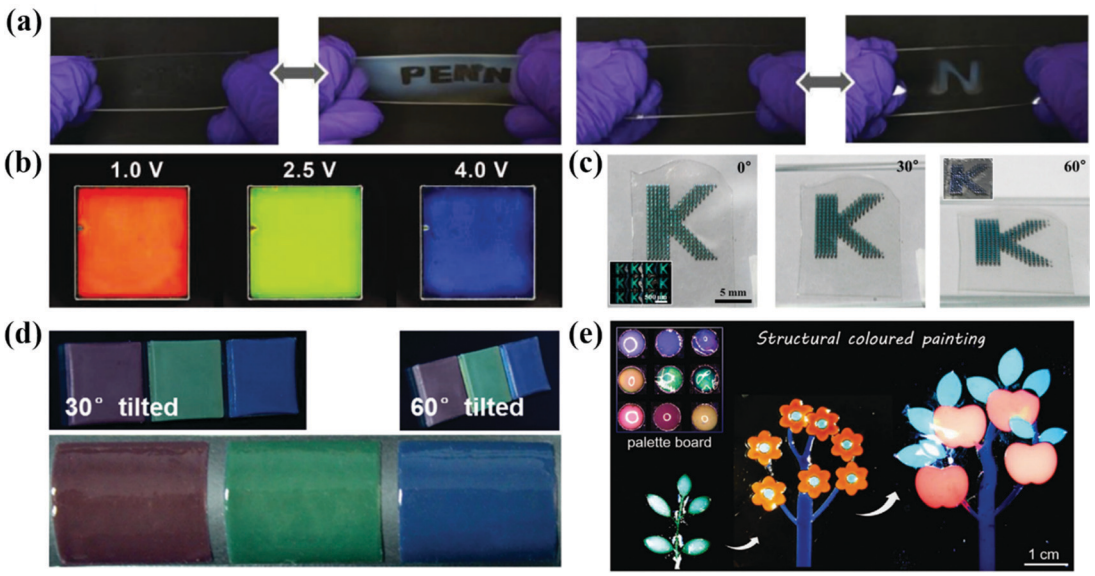

Fig. 12 (a) Optical images of reversible revealing and hiding process of the letters patterned by the silica nanoparticle/PDMS film under stretching and releasing test. (Reproduced with permission.[183] Copyright 2015, Wiley-VCH.) (b) Photographs taken at 1.0 V, 2.5 V and 4.0 V of bias voltages. The pixel size is 5 cm × 5 cm. (Reproduced with permission.[41] Copyright 2010, Wiley-VCH.) (c) Series of optical images of the films containing micropatterns of inverse glasses under diffusive light illumination taken from three different angles, as denoted in each panel. (Reproduced with permission.[184] Copyright 2016, American Chemical Society.) (d) Photographs of the nanocomposite membranes at viewing angles of 30° and 60° from normal to the membrane surface and bended membranes peeled off from the substrates. (Reproduced with permission.[18] Copyright 2017, Wiley-VCH.) (e) Photonic plasticines used as paints for decoration purposes. (Reproduced with permission.[185] Copyright 2021, Wiley-VCH.)

Kim *et al.* dispersed silica colloidal particles in a light-curing resin to form an amorphous arrangement and fixed it by irradiation. After this, the silica particles were removed to obtain an inverse glassy structures.[184] The inverse glasses are an isotropic arrangement of cavities with a low refractive index, thus producing a distinct non-iridescent structural color (Fig. 12c).[184] Zhou *et al.* prepared organogel nanocomposites with a non-iridescent structural color, rapid self-healing properties and self-cleaning ability by co-assembling the monodispersed octadecyl-grafted silica particles and carbon black together with self-healing gels (Fig. 12d).[18] Yu *et al.* synthesized a photonic gel with a non-iridescent structural color, high processability and self-healing ability (Fig. 12e).[185] By adjusting the mechanics of the photonic gel and the size of the internal short-range ordered silica particles, the photonic gel can be processed into bright multicolor patterns.[185]

3.4 Anti-counterfeiting labels

Anti-counterfeiting technologies attract a considerable amount of attention due to their widespread use in banknotes, ID cards, checks and passports.[186–190] APCs can be prepared easily and rapidly by the colloidal suspensions with non-iridescent structural colors. They are easy to process and miniaturize, and have shown great potential for applications in anti-counterfeiting and information encryption when combined with PCs or fluorescent materials.[178,179,191] Specifically, the APC patterns appear or disappear on changing the effective refractive index strength of the assembled structure and their incoherent scattering.[54,85,192] Therefore, APCs offer new approaches to the development of anti-counterfeiting and encryption devices.

Because of the incoherent scattering of the amorphous silica arrays, the thick amorphous arrays always appear white in color regardless of the particle size. Based on this, Takeoka *et al.* sprayed patterns on APCs composed of silica particles in the diameters of 277 nm and 211 nm, where the patterns could not be identified by the naked eye due to strong incoherent scattering.[54] Subsequently, they deposited carbon uniformly on the APC film by pressure-pulsed chemical vapor deposition, and therefore the structural color of APCs gradually showed up as most of the incoherent scattering was absorbed by carbon.[54] Takeoka *et al.* prepared multicolored APC patterns by spraying a silica suspension containing tannic acid (TA) on a piece of white paper. The whole paper was white and the multicolor patterns could not be identified (Fig. 13a).[85] When a solution of iron chloride was sprayed on the patterns, they appeared immediately with visible a color since iron ions react with TA to form black complexes which absorb incoherent scattering.[85] Kim *et al.* prepared polydopamine particle-doped APC elastomers and performed the stretching tests. The structural color turned from blue to brown as the background by stretching because the polydopamine particles were flooded (Fig. 13d)[153] An anti-counterfeiting label based on APCs was prepared by Song and co-workers.[192] In the dry state, the APCs present white color consistent with the middle layer due to incoherent scattering; in the wet state, the middle layer turns transparent and the APC pattern appears due to the absorption of incoherent scattering by the black background which improves the color saturation

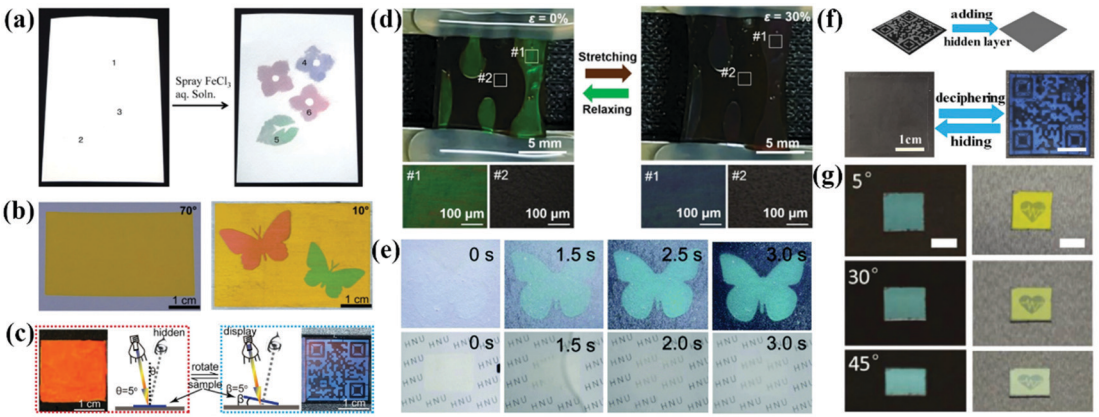

Fig. 13 (a) Left: Whitish sheet obtained using the suspensions composed of silica fine particles of various particle diameters (220, 250, and 300 nm) and TA and dried. Right: Colored diagram obtained by spraying $FeCl_3$ aqueous solution (10 mg mL^{-1}) onto the whitish sheet *via* a mask and drying. (Reproduced with permission.[85] Copyright 2019, American Chemical Society.) (b) Digital photographs of the anti-counterfeiting pattern. The pattern is invisible at the viewing angle of 70° but clearly visible at the viewing angle of 10°. (Reproduced with permission.[51] Copyright 2017, American Chemical Society.) (c) Diagram of the specular reflection mode and the corresponding digital photo of the BLIHS film in red at an incident angle θ of 5°, and diagram of the diffuse reflection mode and the corresponding digital photo in blue with the placement angles β of 5°. (Reproduced with permission.[52] Copyright 2018, American Chemical Society.) (d) A zebra-like pattern at the relaxed state (left panel) and a hidden pattern at the stretched state (right panel). The bottom OM images correspond to the pattern region (#1) and surroundings (#2). (Reproduced with permission.[153] Copyright 2019, American Chemical Society.) (e) Time-lapsed photographs of the anti-counterfeiting label and the intermediate layer being immersed in water. The structural color emerged within 3 s, which was accompanied by the transition into transparency of the intermediate layer. (Reproduced with permission.[192] Copyright 2019, The Royal Society of Chemistry.) (f) Digital photos of QR code encryption and decryption. (Reproduced with permission.[193] Copyright 2020, American Chemical Society.) (g) The optical images of an anti-counterfeiting label captured under natural light and specular reflection illumination at different viewing angles, scale bar: 0.5 cm. (Reproduced with permission.[102] Copyright 2020, Wiley-VCH.)

(Fig. 13e).[192] Tang *et al.* reported a filament film with a single-layer of inverse quasi-amorphous structure.[193] The laminated inverse quasi-amorphous structure based on a silk fibroin film (SFLIS) builds up the water-responsive anti-counterfeiting devices, where SFLIS hides the pattern in air and reveals it when wet (Fig. 13f).[193]

By combining APCs with PCs, anti-counterfeiting labels with unique optical properties can be achieved. Wu *et al.* used monodispersed CdS particles in different diameters as inks to print a waterproof photo paper with vibrant structural colors using an inkjet printer (Fig. 13b).[51] The crystalline arrays of CdS in different diameters were printed on the amorphous arrays of CdS, and invisible anti-counterfeiting patterns can be achieved by a simple rotation angle.[51] Tang *et al.* reported a polyvinylidene fluoride structural color film consisting of the inverse opal structure with ordered array layers and amorphous array layers (Fig. 13c).[52] At a specular reflection angle, the structural color of the amorphous array layer is suppressed by Bragg diffraction and the film displays an iridescent color. Therefore, the patterns on the film are switched between hiding and displaying by changing the observing angles.[52] Zhang *et al.* reported long-range ordered and short-range ordered PS nanoarrays in a PDMS elastomer.[191] When the elastomer was stretched, cracking and surface wrinkling of the PS array reduced the light transmission, thus allowing programmable patterns to be hidden and shown.[191] Duan *et al.* reported a complex anti-counterfeiting encoded composite structure of APCs that combined coherent scattering with the thin film interference (Fig. 13g).[102] Non-iridescent structural colors display in natural light, with bright mixed colors and special reflection under specular lighting.[102]

Our group has developed various strategies for anti-counterfeiting and information storage based on APCs. In the APCs prepared by self-assembly of Y_2O_3 particles, both Y_2O_3 particles and Y_2O_3:Eu particles are easy to assemble into APCs with non-iridescent structural colors due to their instability and high polydispersity. Thus, patterns assembled with these two particles in the same diameter present the same structural color observed by naked eyes.[178] Here, we handwrote the patterning letters with Y_2O_3:Eu particles and the rest letters with the Y_2O_3 particles in the same diameter as background. When irradiated by natural light, these letters show a consistent structural color, while they immediately present red fluorescence under UV illumination. Thus, we successfully constructed a fully reversible hiding-showing pattern by UV irradiation. (Fig. 14a and b). This invisible printing method has the following advantages: (1) the invisible photonic printing is realized based on high contrast of luminous intensity between the pattern and the background other than the structural color and (2) multi-color display can increase the difficulty of identification. In the work on modulating the assembly behavior of colloidal particles by pH value, we developed a new method to construct two photonic microstructures by the assembly of one type of silica particle.[168] More importantly, a coding/decoding system based on the two photonic crystals with different optical properties has been developed by combining APCs with PCs. APCs and PCs with the same stop band were prepared using the solution of aminated silica particles with different pH values. The two films present the same structural color with the same reflective wavelength but different reflection intensities at the viewing angle of 0°. Therefore, by shifting the reflected wavelength to the near infrared region, the color contrast is nearly the same because the human eye is insensitive to near infrared light. As proof-of-concept, we construct a 3 × 3 circular grid with the combination of APCs and PCs at the wavelength of 668 nm. At a viewing angle of 0°, APCs and PCs cannot be identified because of their similar structural colors and low contrast. At other viewing angles, the structural color of APCs remains constant while the structural color of PCs changes, and therefore the APCs are identified (Fig. 14c and d). The coding/decoding system is superior in easily hiding the signal of structural color and combining multiple codes. In our work on assembling the APCs using less polar solvents, a novel system for information storage and identification was developed based on the wetting character of APCs. Their structural colors disappear by wetting due to the reduction of the internal refractive index contrast.[179] A 6-circular-grid system was constructed with APCs whose displaying region

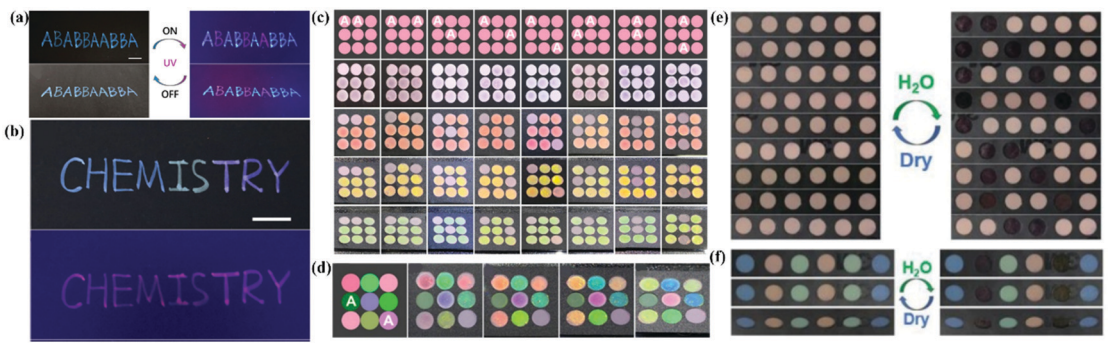

Fig. 14 (a) Invisible photonic printing of the "ABABBAABBA" pattern observed under ambient light and UV light. (b) Invisible photonic printing of a multicolor "Chemistry" pattern under ambient light and UV light. (Reproduced with permission.[178] Copyright 2019, The Royal Society of Chemistry.) (c) Scheme and photos of single color-based coding/decoding systems observed from varied angles. (d) Scheme and photos of multicolor coding and decoding systems observed from varied viewing angles. (Reproduced with permission.[168] Copyright 2020, American Chemical Society.) (e) Digital photos of single-color based coding/decoding system. (f) Digital photos of the multicolor based information storage and recognition system in the dry and wetted states, respectively. (Reproduced with permission.[179] Copyright 2020, Wiley-VCH.)

was hydrophobic after treatment with fluoroalkylsilane and the background remained hydrophilic. The APCs in the hydrophilic background are easily wetted with water along with the disappearance of their structural color, while the structural color of the displaying region remains unchanged (Fig. 14e and f). The displaying region recovered to be invisible after drying and the storage-recognition process showed good reversibility. Similarly, complex information also can be constructed based on the diverse structural colors of APCs. Our group has developed a series of anti-counterfeiting and information storage systems by fully utilizing the unique properties of APCs, such as non-iridescence and high sensitivity to refractive index contrast. We also combine the APCs with fluorescent composites to enhance their practical value as anti-counterfeiting devices.

4. Summary and outlook

We summarize the recent research progress in the preparation strategies, light-absorbing materials and applications of APCs combining the perspective of the self-assembly of colloidal particles into APCs in this review. The preparation methods of APCs are flexible and can be broadly classified into two categories. One is to disturb the equilibrium assembly of the colloidal particles to form an amorphous arrangement by external technical means. The assembly methods include spraying, infiltration-induced colloidal assembly, layer-by-layer deposition and electrophoretic deposition. The other is to weaken the surface potential of the building blocks or change their surface roughness by surface modification or shell coating.[156,166,173] For example, assembly of rough-surface particles, assembly of soft particles and assembly of polymer-grafted particles. Subsequently, we have listed in detail several methods to eliminate the strong incoherent scattering of APCs. The first approach is taking the colloidal particles with a high light absorption capacity and high refractive index as building blocks, including PDA,[194] polysulfide,[38] CdS[51] and Fe_3O_4.[41] The second method is to dope the amorphous array with ferrous materials, *e.g.*, CB,[34,44] graphene,[21,32] PDA,[153] Fe_3O_4,[82] *etc.*[49,75,85] In addition, the incoherent scattering of APCs can be absorbed using black substrates. Finally, various applications of APCs are described, including applications in sensors based on an external stimulus response, structural color printing, wide-view displays, and anti-counterfeit labels.

Although great progress has been made in the preparation of APCs, much efforts are still required for the application of APCs. First, the broad peaks and faint structural colors of APCs limit their application in sensors. For example, the APC-based mechanochromic sensors show a blurry change in the structural color during the deformation of APC elastomers. In contrast, PC sensors have vivid and sensitive change in the structural color. Second, the applications of APCs in displays and printing usually require consideration of durability, compatibility and cost, but most APCs have poor mechanical properties and cannot be recycled. Third, anti-counterfeiting labels based on APCs have excellent mechanical properties and stability,[183,191] and can simply identify the security pattern by stretching or rotating a certain angle.[51,153,168] The solutions to the present challenges of APCs will boost their development and lead to ideal optical devices with unique features and wide applications.

It should be noted that non-iridescent structural colors also can be obtained by particle aggregation that originates from the electromagnetic resonance of the silica particles rather than the scattering of light by the amorphous structures. Recently, our group reported that brilliant non-iridescent structural colors can be fabricated by the random aggregation of large silica particles (300–500 nm). Unlike the conventional non-iridescent structural colors, the new structural color can be attributed to the significant enhancement of electromagnetic resonance by particle aggregation.[195] This work paves a new strategy for the fabrication of unconventional structural colors and will advance their applications in green printing, displays, optical coatings, and wearable devices.

Conflicts of interest

The authors declare no conflict of interest.

Acknowledgements

This work was financially supported by the NSFZJ for Distinguished Young Scholars (LR16B010002), the National Natural Science Foundation of China (21673160, 51372173, 51420105002, 51920105004) and the General Program of the Natural Science Foundation of Guangdong Province (2019A1515011563). Y. Hu and Dr Y. Q. Zhang contributed equally to this work.

References

1 S. John, *Phys. Rev. Lett.*, 1987, **58**, 2486–2489.
2 E. Yablonovitch, *Phys. Rev. Lett.*, 1987, **58**, 2059–2062.
3 J. Hou, M. Li and Y. Song, *Angew. Chem., Int. Ed.*, 2018, **57**, 2544–2553.
4 J. Hou, M. Li and Y. Song, *Nano Today*, 2018, **22**, 132–144.
5 G. Isapour and M. Lattuada, *Adv. Mater.*, 2018, **30**, 1707069.
6 L. Shang, W. Zhang, K. Xu and Y. Zhao, *Mater. Horiz.*, 2019, **6**, 945–958.
7 G. Chen and W. Hong, *Adv. Opt. Mater.*, 2020, **8**, 2000984.
8 P. Wu, J. Wang and L. Jiang, *Mater. Horiz.*, 2020, **7**, 338–365.
9 M. Xiao, M. D. Shawkey and A. Dhinojwala, *Adv. Opt. Mater.*, 2020, **8**, 2000932.
10 H. Yin, B. Dong, X. Liu, T. Zhan, L. Shi, J. Zi and E. Yablonovitch, *Proc. Natl. Acad. Sci. U. S. A.*, 2012, **109**, 10798–10801.
11 L. Shi, Y. Zhang, B. Dong, T. Zhan, X. Liu and J. Zi, *Adv. Mater.*, 2013, **25**, 5314–5320.
12 E. A. Foster, M. A. Jobling, P. G. Taylor, P. Donnelly, P. D. Knijff, R. Miereme, T. Zerjal and C. Tyler Smith, *Nature*, 1998, **396**, 28–29.
13 E. R. Dufresne, H. Noh, V. Saranathan, S. G. J. Mochrie, H. Cao and R. O. Prum, *Soft Matter*, 2009, **5**, 1792–1795.

14 P. W. Anderson, *Phys. Rev.*, 1958, **109**, 1492–1505.
15 B. Q. Dong, X. H. Liu, T. R. Zhan, L. P. Jiang, H. W. Yin, F. Liu and J. Zi, *Opt. Express*, 2010, **18**, 14430–14438.
16 Z. Zhu, J. Zhang, Y. L. Tong, G. Peng, T. Cui, C. F. Wang, S. Chen and D. A. Weitz, *ACS Photonics*, 2019, **6**, 116–122.
17 C. Zhu, W. Xu, L. Chen, W. Zhang, H. Xu and Z. Z. Gu, *Adv. Funct. Mater.*, 2011, **21**, 2043–2048.
18 J. Zhou, P. Han, M. Liu, H. Zhou, Y. Zhang, J. Jiang, P. Liu, Y. Wei, Y. Song and X. Yao, *Angew. Chem., Int. Ed.*, 2017, **56**, 10462–10466.
19 L. Zheng, T. N. T. Tran, D. Zhalmuratova, D. G. Ivey and H. J. Chung, *ACS Appl. Nano Mater.*, 2019, **2**, 6982–6988.
20 Z. Zhang, Z. Chen, L. Sun, X. Zhang and Y. Zhao, *Nano Res.*, 2019, **12**, 1579–1584.
21 Y. Zhang, P. Han, H. Zhou, N. Wu, Y. Wei, X. Yao, J. Zhou and Y. Song, *Adv. Funct. Mater.*, 2018, **28**, 1802585.
22 B. Ye, F. Rong, H. Gu, Z. Xie, Y. Cheng, Y. Zhao and Z. Gu, *Chem. Commun.*, 2013, **49**, 5331–5333.
23 M. Xiao, Y. Li, J. Zhao, Z. Wang, M. Gao, N. C. Gianneschi, A. Dhinojwala and M. D. Shawkey, *Chem. Mater.*, 2016, **28**, 5516–5521.
24 Y. Xia, S. Gao, R. Yu, Z. Zeng, H. He, X. Zhou, Y. Hu, M. Cao and S. Wang, *ACS Appl. Polym. Mater.*, 2021, **3**, 757–764.
25 Y. Xia, S. Gao, H. He, X. Wang, Z. Zeng, B. Chen, N. Zou, M. Cao and S. Wang, *J. Phys. Chem. C*, 2020, **124**, 16083–16089.
26 V. T. Tran, D. K. Lee, J. Kim, J. Lee, L. T. Tufa, D. Pham Cong, C. S. Kim and J. Lee, *Nanoscale*, 2020, **12**, 8453–8465.
27 L. Torres, J. L. Daristotle, O. B. Ayyub, B. M. Bellato Meinhardt, H. Garimella, A. Margaronis, S. Seifert, N. M. Bedford, T. J. Woehl and P. Kofinas, *Nanoscale*, 2019, **11**, 17904–17912.
28 M. Teshima, T. Seki and Y. Takeoka, *Chem. Commun.*, 2018, **54**, 2607–2610.
29 H. Tan, Q. Lyu, Z. Xie, M. Li, K. Wang, K. Wang, B. Xiong, L. Zhang and J. Zhu, *Adv. Mater.*, 2018, **31**, 1805496.
30 Y. Ohtsuka, T. Seki and Y. Takeoka, *Angew. Chem., Int. Ed.*, 2015, **54**, 15368–15373.
31 Z. Liu, Q. Zhang, H. Wang and Y. Li, *J. Colloid Interface Sci.*, 2013, **406**, 18–23.
32 Y. Liu, C. Shao, Y. Wang, L. Sun and Y. Zhao, *Matter*, 2019, **1**, 1581–1591.
33 W. Yuan, N. Zhou, L. Shi and K. Q. Zhang, *ACS Appl. Mater. Interfaces*, 2015, **7**, 14064–14071.
34 K. Katagiri, Y. Tanaka, K. Uemura, K. Inumaru, T. Seki and Y. Takeoka, *NPG Asia Mater.*, 2017, **9**, e355.
35 Q. Zeng, C. Ding, Q. Li, W. Yuan, Y. Peng, J. Hu and K. Q. Zhang, *RSC Adv.*, 2017, **7**, 8443–8452.
36 Q. Li, Y. Zhang, L. Shi, H. Qiu, S. Zhang, N. Qi, J. Hu, W. Yuan, X. Zhang and K. Q. Zhang, *ACS Nano*, 2018, **12**, 3095–3102.
37 Y. Li, L. Chai, X. Wang, L. Zhou, Q. Fan and J. Shao, *Materials*, 2018, **11**, 2500.
38 F. Meng, M. M. Umair, K. Iqbal, X. Jin, S. Zhang and B. Tang, *ACS Appl. Mater. Interfaces*, 2019, **11**, 13022–13028.
39 F. Meng, M. M. Umair, S. Zhang, X. Jin and B. Tang, *J. Mater. Chem. C*, 2019, **7**, 11258–11264.
40 K. Ueno, A. Inaba, Y. Sano, M. Kondoh and M. Watanabe, *Chem. Commun.*, 2009, 3603–3605.
41 I. Lee, D. Kim, J. Kal, H. Baek, D. Kwak, D. Go, E. Kim, C. Kang, J. Chung, Y. Jang, S. Ji, J. Joo and Y. Kang, *Adv. Mater.*, 2010, **22**, 4973–4977.
42 S. Magkiriadou, J. G. Park, Y. S. Kim and V. N. Manoharan, *Opt. Mater. Express*, 2012, **2**, 1343–1352.
43 H. Gu, Y. Zhao, Y. Cheng, Z. Xie, F. Rong, J. Li, B. Wang, D. Fu and Z. Gu, *Small*, 2013, **9**, 2266–2271.
44 Y. Takeoka, S. Yoshioka, A. Takano, S. Arai, K. Nueangnoraj, H. Nishihara, M. Teshima, Y. Ohtsuka and T. Seki, *Angew. Chem., Int. Ed.*, 2013, **52**, 7261–7265.
45 D. Ge, L. Yang, G. Wu and S. Yang, *Chem. Commun.*, 2014, **50**, 2469–2472.
46 N. Koay, I. B. Burgess, T. M. Kay, B. A. Nerger, M. MilesRossouw, T. Shirman, T. L. Vu, G. T. England, K. R. Phillips, S. Utech, N. Vogel, M. Kolle and J. Aizenberg, *Opt. Express*, 2014, **22**, 27750–27768.
47 M. Kuang, J. Wang, B. Bao, F. Li, L. Wang, L. Jiang and Y. Song, *Adv. Opt. Mater.*, 2014, **2**, 34–38.
48 M. Kohri, Y. Nannichi, T. Taniguchi and K. Kishikawa, *J. Mater. Chem. C*, 2015, **3**, 720–724.
49 Y. Zhang, B. Dong, A. Chen, X. Liu, L. Shi and J. Zi, *Adv. Mater.*, 2015, **27**, 4719–4724.
50 F. Wang, X. Zhang, Y. Lin, L. Wang, Y. Qin and J. Zhu, *J. Mater. Chem. C*, 2016, **4**, 3321–3327.
51 S. Wu, B. Liu, X. Su and S. Zhang, *J. Phys. Chem. Lett.*, 2017, **8**, 2835–2841.
52 Y. Meng, J. Qiu, S. Wu, B. Ju, S. Zhang and B. Tang, *ACS Appl. Mater. Interfaces*, 2018, **10**, 38459–38465.
53 M. Sakai, T. Seki and Y. Takeoka, *Small*, 2018, **14**, 1800817.
54 Y. Takeoka, M. Iwata, T. Seki, K. Nueangnoraj, H. Nishihara and S. Yoshioka, *Langmuir*, 2018, **34**, 4282–4288.
55 F. Liu, S. Zhang, X. Jin, W. Wang and B. Tang, *ACS Appl. Mater. Interfaces*, 2019, **11**, 39125–39131.
56 P. Liu, W. Chang, L. Ju, L. Chu, Z. Xie, J. Chen and J. Yang, *ACS Appl. Nano Mater.*, 2019, **2**, 5752–5760.
57 X. Yao, Y. Bai, Y. J. Lee, Z. Qi, X. Liu and Y. Yin, *J. Mater. Chem. C*, 2019, **7**, 14080.
58 P. D. García, R. Sapienza and C. López, *Adv. Mater.*, 2010, **22**, 12–19.
59 P. N. Pusey and W. v. Megen, *Nature*, 1986, **320**, 340–342.
60 P. D. García, R. Sapienza, Á. Blanco and C. López, *Adv. Mater.*, 2007, **19**, 2597–2602.
61 J. D. Forster, H. Noh, S. F. Liew, V. Saranathan, C. F. Schreck, L. Yang, J.-G. Park, R. O. Prum, S. G. J. Mochrie, C. S. O'Hern, H. Cao and E. R. Dufresne, *Adv. Mater.*, 2010, **22**, 2939–2944.
62 M. Harun Ur Rashid, A. Bin Imran, T. Seki, M. Ishii, H. Nakamura and Y. Takeoka, *ChemPhysChem*, 2010, **11**, 579–583.
63 T. F. Wu and J. D. Hong, *Biomacromolecules*, 2015, **16**, 660–666.
64 T. Qiu, B. Luo, F. Ali, E. Jaatinen, L. Wang and H. Wang, *ACS Appl. Mater. Interfaces*, 2016, **8**, 22768–22773.

65 Q. Xu, H. Wang, F. Fu, C. Liu, Z. Chen and Y. Zhao, *J. Nanosci. Nanotechnol.*, 2018, **18**, 4834–4840.
66 G. Chen, B. Yi, Y. Huang, Q. Liang and H. Shen, *Dyes Pigm.*, 2019, **161**, 464–469.
67 J. Hu, X. Lu and J. Gao, *Adv. Mater.*, 2001, **13**, 1708–1712.
68 J. Gao and Z. Hu, *Langmuir*, 2002, **18**, 1360–1367.
69 Y. Takeoka, M. Honda, T. Seki, M. Ishii and H. Nakamura, *ACS Appl. Mater. Interfaces*, 2009, **1**, 982–986.
70 P. N. Dyachenko, J. J. do Rosário, E. W. Leib, A. Y. Petrov, R. Kubrin, G. A. Schneider, H. Weller, T. Vossmeyer and M. Eich, *ACS Photonics*, 2014, **1**, 1127–1133.
71 D. Ge, L. Yang, G. Wu and S. Yang, *J. Mater. Chem. C*, 2014, **2**, 4395–4400.
72 S. Yoshioka and Y. Takeoka, *ChemPhysChem*, 2014, **15**, 2209–2215.
73 F. Wang, X. Zhang, L. Zhang, M. Cao, Y. Lin and J. Zhu, *Dyes Pigm.*, 2016, **130**, 202–208.
74 L. Bai, V. C. Mai, Y. Lim, S. Hou, H. Möhwald and H. Duan, *Adv. Mater.*, 2018, **30**, 1705667.
75 R. Hirashima, T. Seki, K. Katagiri, Y. Akuzawa, T. Torimoto and Y. Takeoka, *J. Mater. Chem. C*, 2014, **2**, 344–348.
76 M. Teshima, T. Seki, R. Kawano, S. Takeuchi, S. Yoshioka and Y. Takeoka, *J. Mater. Chem. C*, 2015, **3**, 769–777.
77 P. Liu, X. Liu, M. Ji, H. Gu, C. Zhou, L. Lei, J. Lu, X. Wu, T. Zhu and J. Yang, *J. Colloid Interface Sci.*, 2020, **580**, 573–582.
78 N. Zhou, A. Zhang, L. Shi and K. Q. Zhang, *ACS Macro Lett.*, 2013, **2**, 116–120.
79 J. Hyon, C. Seo, I. Yoo, S. Song and Y. Kang, *Sens. Actuators, B*, 2016, **223**, 878–883.
80 K. Katagiri, K. Uemura, R. Uesugi, K. Inumaru, T. Seki and Y. Takeoka, *RSC Adv.*, 2018, **8**, 10776–10784.
81 S. H. Kim, S. J. Jeon, W. C. Jeong, H. S. Park and S. M. Yang, *Adv. Mater.*, 2008, **20**, 4129–4134.
82 Y. Takeoka, S. Yoshioka, M. Teshima, A. Takano, M. Harun Ur Rashid and T. Seki, *Sci. Rep.*, 2013, **3**, 2371.
83 C. H. Lim, H. Kang and S. H. Kim, *Langmuir*, 2014, **30**, 8350–8356.
84 N. Sun, X. Liu, Y. Liu, R. Zhao, Z. Xu, S. Li, J. Lian, Q. Jiang and G. Wang, *Nanoscale Adv.*, 2020, **2**, 4581–4590.
85 M. Sakai, T. Seki and Y. Takeoka, *ACS Sustainable Chem. Eng.*, 2019, **7**, 14933–14940.
86 H. Shen, Q. Liang, L. Song, G. Chen, Y. Pei, L. Wu and X. Zhang, *J. Mater. Sci.*, 2019, **55**, 2353–2364.
87 X. Shi, J. He, L. Wu, S. Chen and X. Lu, *J. Coat. Technol. Res.*, 2020, **17**, 1033–1042.
88 S. J. Lee, J. W. Choi, S. Kumar, C. L. Lee and J. S. Lee, *Mater. Horiz.*, 2018, **5**, 1120–1129.
89 P. Liu, J. Chen, Z. Zhang, Z. Xie, X. Du and Z. Gu, *Nanoscale*, 2018, **10**, 3673–3679.
90 J. Bi, S. Wu, H. Xia, L. Li and S. Zhang, *J. Mater. Chem. C*, 2019, **7**, 4551–4558.
91 Y. Xue, F. Wang, H. Luo and J. Zhu, *ACS Appl. Mater. Interfaces*, 2019, **11**, 34355–34363.
92 D. Allard, B. Lange, F. Fleischhaker, R. Zentel and M. Wulf, *Soft Mater.*, 2005, **3**, 121–131.
93 L. Cui, Y. Zhang, J. Wang, Y. Ren, Y. Song and L. Jiang, *Macromol. Rapid Commun.*, 2009, **30**, 598–603.
94 G. H. Lee, S. H. Han, J. B. Kim, D. J. Kim, S. Lee, W. M. Hamonangan, J. M. Lee and S. H. Kim, *ACS Appl. Polym. Mater.*, 2019, **2**, 706–714.
95 Y. Feng, J. Sun, L. Xu and W. Hong, *Adv. Mater. Interfaces*, 2021, **8**, 2001950.
96 Y. Naoi, T. Seki, R. Ohnuki, S. Yoshioka and Y. Takeoka, *Langmuir*, 2019, **35**, 13983–13990.
97 F. Wang, F. Guo, Y. Xue, H. Luo and J. Zhu, *J. Coat. Technol. Res.*, 2020, **18**, 489–499.
98 Y. Xue, F. Wang, Y. Qin, B. Lu, L. Wang and J. Zhu, *Langmuir*, 2019, **35**, 6956–6961.
99 V. J. Anderson and H. N. W. Lekkerkerker, *Nature*, 2002, **416**, 811–815.
100 H. Hu and R. G. Larson, *Langmuir*, 2005, **21**, 3972–3980.
101 L. Bai, Y. He, J. Zhou, Y. Lim, V. C. Mai, Y. Chen, S. Hou, Y. Zhao, J. Zhang and H. Duan, *Adv. Opt. Mater.*, 2019, **7**, 1900522.
102 L. Bai, Y. Lim, Y. He, Q. Xiong, S. Hou, J. Zhang and H. Duan, *Adv. Opt. Mater.*, 2020, **8**, 2001378.
103 J. J. Richardson, M. Bjornmalm and F. Caruso, *Science*, 2015, **348**, aaa2491.
104 K. Katagiri, S. I. Yamazaki, K. Inumaru and K. Koumoto, *Polym. J.*, 2014, **47**, 190–194.
105 K. W. Tan, G. Li, Y. K. Koh, Q. Yan and C. C. Wong, *Langmuir*, 2008, **24**, 9273–9278.
106 K. Ariga, J. P. Hill and Q. Ji, *Phys. Chem. Chem. Phys.*, 2007, **9**, 2319–2340.
107 R. K. Iler, *J. Colloid Interface Sci.*, 1966, **21**, 569–594.
108 M. Iwata, M. Teshima, T. Seki, S. Yoshioka and Y. Takeoka, *Adv. Mater.*, 2017, **29**, 1605050.
109 K. L. Wu and S. K. Lai, *Langmuir*, 2005, **21**, 3238–3246.
110 M. Teshima, M. Suzuki, T. Seki and Y. Takeoka, *ChemNanoMat*, 2018, **4**, 621–625.
111 Y. Hu, D. Yang and S. Huang, *ACS Omega*, 2019, **4**, 18771–18779.
112 M. Trau, D. A. Saville and I. A. Aksay, *Science*, 1996, **272**, 706–709.
113 R. C. Hayward, D. A. Saville and I. A. Aksay, *Nature*, 2000, **404**, 56–59.
114 P. V. Braun and P. Wiltzius, *Curr. Opin. Colloid Interface Sci.*, 2002, **7**, 116–123.
115 W. Wang, A. Zheng, Y. Jiang, D. Lan, F. Lu, L. Zheng, L. Zhuang and R. Hong, *RSC Adv.*, 2019, **9**, 498–506.
116 S. J. Yuan, W. H. Meng, A. H. Du, X. Y. Cao, Y. Zhao, J. X. Wang and L. Jiang, *Chin. J. Polym. Sci.*, 2019, **37**, 729–736.
117 Z. Yang, G. Chen, Y. Huang, Q. Liang and H. Shen, *Surf. Interfaces*, 2021, **24**, 101045.
118 N. Kumano, T. Seki, M. Ishii, H. Nakamura and Y. Takeoka, *Angew. Chem., Int. Ed.*, 2011, **50**, 4012–4015.
119 N. Kumano, T. Seki, M. Ishii, H. Nakamura, T. Umemura and Y. Takeoka, *Adv. Mater.*, 2011, **23**, 884–888.
120 P. Han, X. He, Y. Zhang, H. Zhou, M. Liu, N. Wu, J. Jiang, Y. Wei, X. Yao, J. Zhou and Y. Song, *Adv. Opt. Mater.*, 2019, **7**, 1801749.

121 S. H. Kim, J. G. Park, T. M. Choi, V. N. Manoharan and D. A. Weitz, *Nat. Commun.*, 2014, **5**, 3068.
122 J. G. Park, S. H. Kim, S. Magkiriadou, T. M. Choi, Y. S. Kim and V. N. Manoharan, *Angew. Chem., Int. Ed.*, 2014, **53**, 2899–2903.
123 T. H. Zhao, G. Jacucci, X. Chen, D. P. Song, S. Vignolini and R. M. Parker, *Adv. Mater.*, 2020, **32**, 2002681.
124 S. H. Kim, S. H. Kim and S. M. Yang, *Adv. Mater.*, 2009, **21**, 3771–3775.
125 H. S. Lee, J. H. Kim, J. S. Lee, J. Y. Sim, J. Y. Seo, Y. K. Oh, S. M. Yang and S. H. Kim, *Adv. Mater.*, 2014, **26**, 5801–5807.
126 J. H. Moon, G. R. Yi, S. M. Yang, D. J. Pine and S. B. Park, *Adv. Mater.*, 2004, **16**, 605–609.
127 J. Y. Sim, J. H. Choi, J. M. Lim, S. Cho, S. H. Kim and S. M. Yang, *Small*, 2014, **10**, 3979–3985.
128 S. H. Kim, S. Y. Lee, G. R. Yi, D. J. Pine and S. M. Yang, *J. Am. Chem. Soc.*, 2006, **128**, 10897–10904.
129 C. Kim, K. Jung, J. W. Yu, S. Park, S. H. Kim, W. B. Lee, H. Hwang, V. N. Manoharan and J. H. Moon, *Chem. Mater.*, 2020, **32**, 9704–9712.
130 J. B. Kim, S. Y. Lee, N. G. Min, S. Y. Lee and S. H. Kim, *Adv. Mater.*, 2020, **32**, 2001384.
131 R. Ohnuki, M. Sakai, Y. Takeoka and S. Yoshioka, *Langmuir*, 2020, **36**, 5579–5587.
132 J. B. K. Seong Kyeong Nam, S. H. Han and S. H. Kim, *ACS Nano*, 2020, **14**, 15714–15722.
133 M. Sakai, H. Kim, Y. Arai, T. Teratani, Y. Kawai, Y. Kuwahara, K. Abe, Y. Kuwana, K. Ikeda, K. Yamada and Y. Takeoka, *ACS Appl. Nano Mater.*, 2020, **3**, 7047–7056.
134 R. Ohnuki, S. Isoda, M. Sakai, Y. Takeoka and S. Yoshioka, *Adv. Opt. Mater.*, 2019, **7**, 1900227.
135 T. M. Choi, J. G. Park, Y. S. Kim, V. N. Manoharan and S. H. Kim, *Chem. Mater.*, 2015, **27**, 1014–1020.
136 X. Chen, X. Yang, D. P. Song, Y. F. Men and Y. Li, *Macromolecules*, 2021, **54**, 3668–3677.
137 Y. L. Li, X. Chen, H. K. Geng, Y. Dong, B. Wang, Z. Ma, L. Pan, G. Q. Ma, D. P. Song and Y. S. Li, *Angew. Chem., Int. Ed.*, 2020, **60**, 3647–3653.
138 Q. J. Liu, Y. Li, J. C. Xu, H. F. Lu, Y. Li and D. P. Song, *ACS Nano*, 2021, **15**, 5534–5544.
139 H. Gu, B. Ye, H. Ding, C. Liu, Y. Zhao and Z. Gu, *J. Mater. Chem. C*, 2015, **3**, 6607–6612.
140 S. J. Yeo, F. Tu, S. H. Kim, G. R. Yi, P. J. Yoo and D. Lee, *Soft Matter*, 2015, **11**, 1582–1588.
141 R. P. Sear, *Europhys. Lett.*, 1998, **44**, 531–535.
142 D. S. Choi, J. H. Choi and C. Y. Lee, *Appl. Sci.*, 2020, **10**, 420.
143 J. K. Pi, J. Yang, Q. Zhong, M. B. Wu, H. C. Yang, M. Schwartzkopf, S. V. Roth, P. Müller Buschbaum and Z. K. Xu, *ACS Appl. Nano Mater.*, 2019, **2**, 4556–4566.
144 M. Xiao, Z. Hu, Z. Wang, Y. Li, A. D. Tormo, N. L. Thomas, B. Wang, N. C. Gianneschi, M. D. Shawkey and A. Dhinojwala, *Sci. Adv.*, 2017, **3**, e1701151.
145 K. Ohno and Y. Mizuta, *ACS Appl. Polym. Mater.*, 2019, **2**, 368–375.
146 S. H. Kim, S. Magkiriadou, D. K. Rhee, D. S. Lee, P. J. Yoo, V. N. Manoharan and G. R. Yi, *ACS Appl. Mater. Interfaces*, 2017, **9**, 24155–24160.
147 G. H. Lee, J. B. Kim, T. M. Choi, J. M. Lee and S. H. Kim, *Small*, 2019, **15**, 1804548.
148 M. Xiao, Z. Hu, T. E. Gartner III, X. Yang, W. Li, A. Jayaraman, N. C. Gianneschi, M. D. Shawkey and A. Dhinojwala, *Sci. Adv.*, 2019, **5**, eaax1254.
149 T. Iwasaki, S. Harada, T. Okoshi, M. Moriya, T. Kojima, K. Kishikawa and M. Kohri, *Langmuir*, 2020, **36**, 11880–11887.
150 D. Yang, G. Liao and S. Huang, *Langmuir*, 2019, **35**, 8428–8435.
151 Y. Cui, F. Wang, J. Zhu, W. Wu, Y. Qin and X. Zhang, *J. Colloid Interface Sci.*, 2018, **531**, 609–617.
152 L. Song, X. Chen, Y. Xie, L. Zhong, X. Zhang and Z. Cheng, *Dyes Pigm.*, 2019, **164**, 222–226.
153 G. H. Lee, S. H. Han, J. B. Kim, J. H. Kim, J. M. Lee and S. H. Kim, *Chem. Mater.*, 2019, **31**, 8154–8162.
154 X. Yang, D. Ge, G. Wu, Z. Liao and S. Yang, *ACS Appl. Mater. Interfaces*, 2016, **8**, 16289–16295.
155 D. Ge, X. Yang, Z. Chen, L. Yang, G. Wu, Y. Xia and S. Yang, *Nanoscale*, 2017, **9**, 17357–17363.
156 A. Kawamura, M. Kohri, G. Morimoto, Y. Nannichi, T. Taniguchi and K. Kishikawa, *Sci. Rep.*, 2016, **6**, 33984.
157 B. Yi and H. Shen, *J. Mater. Chem. C*, 2017, **5**, 8194–8200.
158 B. Yi and H. Shen, *Appl. Surf. Sci.*, 2018, **427**, 1129–1136.
159 T. Iwasaki, Y. Tamai, M. Yamamoto, T. Taniguchi, K. Kishikawa and M. Kohri, *Langmuir*, 2018, **34**, 11814–11821.
160 L. Bai, Y. Lim, J. Zhou, L. Liang and H. Duan, *Langmuir*, 2019, **35**, 9878–9884.
161 Y. Häntsch, G. Shang, A. Petrov, M. Eich and G. A. Schneider, *Adv. Opt. Mater.*, 2019, **7**, 1900428.
162 M. Kohri, Y. Tamai, A. Kawamura, K. Jido, M. Yamamoto, T. Taniguchi, K. Kishikawa, S. Fujii, N. Teramoto, H. Ishii and D. Nagao, *Langmuir*, 2019, **35**, 5574–5580.
163 T. Okada, S. Hosoyamada, C. Takada and C. Ohta, *ChemPhotoChem*, 2020, **5**, 32–35.
164 J. D. Debord and L. A. Lyon, *J. Phys. Chem. B*, 2000, **104**, 6327–6331.
165 T. Hellweg, C. D. Dewhurst, E. BruÈckner, K. Kratz and W. Eimer, *Colloid Polym. Sci.*, 2000, **278**, 972–978.
166 Y. Gotoh, H. Suzuki, N. Kumano, T. Seki, K. Katagiri and Y. Takeoka, *New J. Chem.*, 2012, **36**, 2171–2175.
167 K. Ueno, A. Inaba, T. Ueki, M. Kondoh and M. Watanabe, *Langmuir*, 2010, **26**, 18031–18038.
168 D. Yang, Y. Hu, Y. Hu and S. Huang, *J. Phys. Chem. C*, 2020, **124**, 6328–6336.
169 M. Kohri, K. Uradokoro, Y. Nannichi, A. Kawamura, T. Taniguchi and K. Kishikawa, *Photonics*, 2018, **5**, 36.
170 M. Liu, W. Jian, S. Wang, S. Xuan, L. Bai, M. Sang and X. Gong, *Smart Mater. Struct.*, 2018, **27**, 095012.
171 W. S. Jinn, M. K. Shin, B. Kang, S. Oh, C. E. Moon, B. Mun, Y. W. Ji, H. K. Lee and S. Haam, *J. Mater. Chem. B*, 2019, **7**, 7120–7128.
172 Y. S. Kazuhide Ueno, Aya Inaba, Masashi Kondoh and Masayoshi Watanabe, *J. Phys. Chem. B*, 2010, **114**, 13095–13103.

173 K. Ueno and M. Watanabe, *Langmuir*, 2011, **27**, 9105–9115.
174 C. Zhou, Y. Qi, S. Zhang, W. Niu, W. Ma, S. Wu and B. Tang, *Dyes Pigm.*, 2020, **176**, 108226.
175 S. Y. Lee, H. Kim, S. H. Kim and H. A. Stone, *Phys. Rev. Appl.*, 2018, **10**, 054003.
176 H. Shen, Q. Liang, L. Song, G. Chen, Y. Pei, L. Wu and X. Zhang, *J. Mater. Sci.*, 2020, **55**, 2353–2364.
177 D. Yang, W. Luo, Y. Huang and S. Huang, *ACS Omega*, 2019, **4**, 528–534.
178 D. Yang, G. Liao and S. Huang, *J. Mater. Chem. C*, 2019, **7**, 11776–11782.
179 X. Yang, D. Yang, Y. Chen, Y. Hu and S. Huang, *Part. Part. Syst. Charact.*, 2020, **37**, 2000043.
180 M. Li, H. Tan, L. Jia, R. Zhong, B. Peng, J. Zhou, J. Xu, B. Xiong, L. Zhang and J. Zhu, *Adv. Funct. Mater.*, 2020, **30**, 2000008.
181 M. Li, B. Zhou, Q. Lyu, L. Jia, H. Tan, Z. Xie, B. Xiong, Z. Xue, L. Zhang and J. Zhu, *Mater. Chem. Front.*, 2019, **3**, 2707–2715.
182 X. Zhang, Y. Ran, Q. Fu and J. Ge, *J. Mater. Chem. C*, 2020, **8**, 17202–17210.
183 D. Ge, E. Lee, L. Yang, Y. Cho, M. Li, D. S. Gianola and S. Yang, *Adv. Mater.*, 2015, **27**, 2489–2495.
184 G. H. Lee, J. Y. Sim and S. H. Kim, *ACS Appl. Mater. Interfaces*, 2016, **8**, 12473–12480.
185 J. Zhang, J. Zhang, Y. Ou, Y. Qin, H. Wen, W. Dong, R. Wang, S. Chen and Z. Yu, *Small*, 2021, **17**, 2007426.
186 B. Hardwick, W. Jackson, G. Wilson and A. W. H. Mau, *Adv. Mater.*, 2001, **13**, 980–984.
187 A. Mullard, *Nat. Med.*, 2010, **16**, 361.
188 E. L. Prime and D. H. Solomon, *Angew. Chem.*, 2010, **122**, 3814–3824.
189 E. L. Prime and D. H. Solomon, *Angew. Chem., Int. Ed.*, 2010, **49**, 3726–3736.
190 B. Yoon, J. Lee, I. S. Park, S. Jeon, J. Lee and J. M. Kim, *J. Mater. Chem. C*, 2013, **1**, 2388–2403.
191 Y. Qi, C. Zhou, S. Zhang, Z. Zhang, W. Niu, S. Wu, W. Ma and B. Tang, *Dyes Pigm.*, 2021, **189**, 109264.
192 X. He, Y. Gu, B. Yu, Z. Liu, K. Zhu, N. Wu, X. Zhao, Y. Wei, J. Zhou and Y. Song, *J. Mater. Chem. C*, 2019, **7**, 14069–14074.
193 Z. Wang, F. Meng, S. Zhang, Y. Meng, S. Wu and B. Tang, *ACS Appl. Mater. Interfaces*, 2020, **12**, 56413–56423.
194 B. Yi and H. Shen, *Chem. Commun.*, 2017, **53**, 9234–9237.
195 B. Li, C. Ouyang, D. Yang, Y. Ye, D. Ma, L. Luo and S. Huang, *J. Colloid Interface Sci.*, 2021, **604**, 178–187.